# DEVELOPMENT OF A RAPID DIAGNOSTIC TEST FOR DETECTION OF *STREPTOCOCCUS MUTANS* IN ORAL FLUIDS FOR THE DIAGNOSIS OF DENTAL CARIES

By:

Kelly L. Braddock, B.S.

A thesis submitted to the Graduate Council of
Texas State University in partial fulfillment
of the requirements for the degree of Master of Science
with a Major in Biology
December 2017

Committee Members:

Shannon Weigum, Chair

Robert McLean

John Carrano

## FAIR USE AND AUTHORS'S PERMISSION STATEMENT

### Fair Use



### Duplication Permission

**ACKNOWLEDGEMENTS**

First, I would like to express my sincere gratitude for my advisor, Dr. Shannon Weigum, for her continuous mentorship and support. Her guidance, motivation, and patience were extremely valuable throughout my graduate career. I am so grateful to have had an advisor who provided motivation and knowledge, both professionally and academically, that, I have, and likely will continue to benefit from.

I would also like to thank Dr. Mc Lean for his insightful advice and support and Dr. Carrano for his continued encouragement and the opportunity to join the team at Paratus Diagnostics working as an intern.

## TABLE OF CONTENTS

**Page**

## LIST OF TABLES

**Table** **Page**

## LIST OF FIGURES

**Figure** **Page**

## LIST OF ABBREVIATIONS

| Abbreviation | Description |
|---|---|
| A280 | Absorbance at 280nm |
| ATR | Acid tolerance response |
| BHI | Brain heart infusion media |
| BrpA | Biofilm regulatory protein A |
| BSA | Bovine serum albumin |
| CBP | Collagen binding protein |
| CFU | colony forming unit |
| CMB | Cerebral microbleed |
| DI water | deionized water |
| GTF | Glucosyl transferase |
| GAM | Goat- anti mouse antibody (positive control) |
| HRP | Horse radish peroxidase |
| IBD | Irritable bowel disease |
| IE | Infective endocarditis |
| IgG | Immunoglobulin G |
| IL | Interleukin protein |
| kDa | Kilodaltons |
| LFA | Lateral flow assay |
| LOD | Limit of detection |
| LOQ | Limit of quantitation |
| MCP-1 | Monocyte chemoattractant protein 1 |
| OD | Optical density |
| PAc | Protein antigen c |

| | |
|---|---|
| PBS | 0.1M phosphate buffered saline |
| PBST | 0.1M PBS with specified tween 20 concentration |
| PES | Polyethersulfone |
| Strep-HRP | Streptavidin-HRP conjugate |
| TLR | Toll-like receptors |

## ABSTRACT

The personal and financial impact of common and often overlooked oral diseases, such as dental caries, is sizable and prevalent throughout the world. Rapid diagnostic tools continue to be developed to prevent, diagnose and monitor treatment responses of a variety of diseases including, dental caries. This assay, like many other point-of-care diagnostics, is based on the lateral flow immunoassay design. Initial development required identification of two antibodies that specifically recognize antigens on the surface of *Streptococcus mutans*, and are compatible as a matched pair. To identify a matched pair, antibodies were first purified from hybridoma cell culture supernatant, by affinity chromatography, and screened against two *S. mutans* strains of differing serotypes. The two hybridoma cell lines for which antibody was successfully purified, were screened and both indicated activity against one *S. mutans* strain of the most common serotype, serotype *c*. However, only one of the purified antibodies was able to recognize the non-serotype *c* strain. Further assay development focused only on the strain of *S. mutans* recognized by both antibodies. Conjugation to biotin allows the detection antibody to form a complex with the reporter molecule HRP, which is conjugated to streptavidin. A portion of both antibody stocks were conjugated to biotin and each of them was tested in both the detecting and capture positions, in order to determine the optimal orientation of the matched pair. Only one orientation recognized *S. mutans* within the lateral flow assay. Initial experiments indicated that the lower limit for *S. mutans* detection was within the clinically relevant range, for which concentration of salivary *S. mutans* can be used to diagnose dental caries. After identifying a matched pair, detergent concentration as well as blocking conditions were optimized. To assess analytical performance within a realistic matrix, a dose response curve was created from samples made in human pooled saliva. The dose response indicated results of the assay at varying concentrations were reproducible, but detection of *S. mutans* occurred only at concentrations much higher than in previous testing. This discrepancy is likely due to matrix effects within saliva, including presence of endogenous proteins and high viscosity. Future testing to optimize the assay within saliva, may improve its detection capabilities by mitigating some of these matrix effects, through addition of detergents or mucolytic agents.

# 1 INTRODUCTION

## 1.1 Oral disease statistics and impact

Dental caries, commonly known as cavities, are not only a source of great discomfort for many, but can lead to more serious infections and reduced functionality, which lowers nutritional content and quality of life. *Streptococcus* are the most common bacterial species that can cause dental caries and can become the source of infective endocarditis, an infection of the endocardium, or inner lining of the heart [1]. According to the WHO, 60-90% of school children experience dental caries in industrialized countries with oral health related costs accounting for 5-10% of all healthcare expenses in these areas [2]. Those that have adopted a preventive rather than a curative approach to oral health have seen a reduction in oral healthcare costs [2].

In the developing world, the limited availability of tests and imaging techniques commonly used in developed nations, is a major impediment to proper oral healthcare monitoring and treatment. To improve patient outcomes, careful consideration of individual factors that impede access to care, is vital. The number of general healthcare facilities is low, but there are even fewer oral health care providers, and the persistent need for these services has given rise to non-dental professionals and even individuals with no medical background, attempting to administer oral healthcare [3]. Unfortunately, the actions of these well-intentioned “care providers” have been linked to the spread of infectious disease[3]. Even in areas with laboratory facilities capable of administering diagnostic tests, they are often too expensive, especially when lengthy travel times often cut significantly into much needed daily earnings[4]. The long distances that must be travelled also deter return visits, which is usually the first opportunity to provide a more tailored treatment plan, due to the time required to run diagnostic tests from the initial visit. Many of the reagents used in traditional diagnostics are time and temperature sensitive. Short shelf-life and cost of temperature controlled transportation and storage contribute to the high price of conventional diagnostics [4]. While the occurrence of oral diseases is high in

both industrialized and developing countries, reduced accessibility to oral healthcare services in developing countries results in patient outcomes that are often less favorable [5].

## 1.2 Lateral flow devices for point-of-care diagnostics

As with many diseases, early diagnosis and treatment are critical for improved patient outcomes. In developing countries, many of the impediments to accessible care are due to the high cost of the treatment itself, as well as the long distances that often must be traveled to reach the nearest health care provider. Although there are better outcomes overall in developed countries, these issues also exist to a certain extent in developed countries including in the U.S. where annual treatment costs for tooth decay alone have been in the billions for decades and continue to increase every year [6]. These factors highlight the need for cost-effective, early diagnosis in both settings. Point-of-care diagnostics are aimed at mitigating these problems through development of low cost, rapid diagnostic tools that can be used without the need of highly trained professionals and allow for a tailored treatment plan to be administered on the initial visit. Lateral flow devices are one of the most common platforms for point-of-care diagnostics, the most ubiquitous of these is the pregnancy test stick. The development of a lateral flow immunoassay (LFIA) for HIV diagnosis has improved patient outcomes through early detection [5, 7]. In 2010, more than 29 million people in developing countries were tested for HIV, many of them were pregnant women who could begin anti-retroviral treatment in time to prevent mother-to-infant transmission[5]. These same technologies could also prove to be highly beneficial for oral health diagnosis and monitoring.

## 1.3 *Streptococcus mutans* and dental caries

*S. mutans* is the bacterial species most commonly associated with dental caries and although it is also found in healthy individuals, it is present in significantly higher levels when

tooth decay is occurring [8]. The main source of its virulence in the oral cavity is its ability to produce acids near the enamel surface. The fermentation of carbohydrates by *S. mutans* and other bacteria within the plaque, lowers acidity causing enamel demineralization. *S. mutans* expresses surface-attached and secreted glucosyltransferases (GTF), enzymes that produce glucans derived from sugars, with sucrose being their preferred substrate[9]. Together GTFs and glucans mediate adhesion of bacteria to the enamel surface and to other bacteria[10]. Glucans also play a major role in triggering the acid tolerance response (ATR), which is also vital to their cariogenicity [11]. At low pH, protons accumulate on the surface of insoluble glucans promoting upregulation of genes involved in the ATR [11].

The strains of *S. mutans* are divided into serotypes based on their surface antigens. The most commonly found serotype in the oral cavity is serotype *c*; while serotype *e;* is the next most abundant, its distribution is significantly smaller; and serotypes *f* and *k* are very rare [12]. There is no strong evidence for one specific serotype correlating more strongly to caries development, but the presence of multiple serotypes with non-c serotypes making up a noticeably larger portion of the total serotype distribution, is linked to increased caries risk. This highlights the importance of species, but not serotype specific detection for developers of diagnostic tools and sensitivity for non-c serotypes should be assessed as part of the development process [13].

Salivary levels of *S. mutans* associated with high caries activity are $>10^6$ CFU/ml, and concentrations seen with low caries activity are around $10^5$ CFU/ml or lower [14]. An LOD (limit of detection) around $5x10^5$ provides the sensitivity to detect most moderate to severe carious activity and minimizes the occurrence of false positives. Similar diagnostic tests have also designated the same cut-off value for detection of clinically relevant concentrations of *S. mutans* [15]. Although concentrations would be much higher in plaque, for lateral flow assays to truly be point-of-care, the sample to be tested should readily flow across the test strip without manipulation to the sample.

## 1.4 Oral bacteria colonization

*S. mutans* is just one species of more than 500 present within dental plaque [16]. Not all oral bacteria are able to attach directly to the tooth, but those that can, known as early colonizers, serve as a means of attachment for subsequent species to colonize. The early colonizers usually have an advantage in attaching to the tooth surface. For example, IgA antibodies in the saliva inhibit bacterial adherence to the tooth, but some early colonizers overcome this by secreting IgA proteases [17]. Through coadhesdion two distinct species, one planktonic and one surface attached, recognize and bind one another, the mechanism of recognition is the same between two planktonic species but is termed coaggregation [18]. All species of the oral microbiome have the ability to coaggregate/ coadhere with at least one, but usually many other species, allowing a large variety of bacteria to colonize the surface of the tooth and contributing to the formation of biofilms [19].

## 1.5 Dental caries pathology

Healthy individuals experience low enamel acidity, but when pH is lowered, for example due to frequent sugar consumption, the enamel surface becomes acidic due to the production of bacterial fermentative waste products and their accumulation selects for the same acid tolerant bacteria like *S. mutans*. Prolonged enamel acidity leads to enamel demineralization: the initial step in formation of dental caries. When these acidic conditions remain after significant demineralization, dental decay begins. With the inorganic matrix of the teeth removed through demineralization, the organic matrix is easily accessible to host proteases that are activated at low pH and begin to degrade structural proteins of the organic matrix.

The occurrence of dental caries is much higher in patients that currently or have previously suffered from chronic periodontitis [20]. *S. mutans* remains on the enamel surface adjacent to periodontal infections and increased levels of *S. mutans* on the enamel during

periodontal infections increases the risk of developing caries[20]. In both saliva and sub-gingival plaque, increased concentrations of *S. mutans* are seen in many cases of chronic periodontal infections, suggesting that the conditions created by periodontitis may produce a favorable environment for proliferation of *S. mutans* and could explain the high incidences of carious lesions during or soon after periodontal infections [21]. Methods for detecting high levels of *S. mutans* during initial periodontal treatment would give care providers the opportunity to be proactive and reduce their patient's risk of developing dental caries. A point-of-care diagnostic capable of detecting high levels of *S. mutans* would permit the diagnosis of dental caries and may even help to determine a periodontal patient's risk of developing caries.

The altered oral environment caused by decay and periodontitis is in part due to activation of host proteases responsible for degradation of host tissues and the progression of disease. Oral pathogens have proteases as well, however the majority of both dentin and soft tissue damage is attributed to host proteases that become activated at low pH [22, 23]. The large majority of these enzymes are part of a group of host proteases known as matrix metalloproteinases (MMPs). This class of proteases break down the extracellular matrix of soft and hard tissues, largely composed of collagen type I. Collagen type I is difficult to degrade and salivary collagenolytic proteases are rare outside of this unique class of proteinases. MMP-8 is the major host protease in dentin and carries out the majority of hard tissue degradation [24]. Salivary concentrations of these destructive host proteases are increased with the onset of dental caries [25-28].

### 1.6 *S. mutans* and the oral systemic disease connection

Although *S. mutans* is commonly found as an oral commensal and is the most common species found in caries associated dental plaque, the evidence for its pathogenicity elsewhere in the body is growing [6, 29]. Interestingly many of the strains isolated from extra-oral sites display

features that are not common within the oral cavity, suggesting differential genome content and/or expression is beneficial in colonizing host tissues outside of the oral cavity. Phenotypic variation within *S. mutans* motivated researchers to further subdivide them into serotypes, but even within serotypes there is considerable variation and virulence outside of the oral cavity is very strain specific [30]. More recently those phenotypic differences have been confirmed with genomic alterations, many of which seem to be the result of gene deletions and presence of foreign DNA, suggesting flexibility in the genome [31]. Most systemic diseases influenced by *S. mutans* involve enhancement of inflammation to diseases that are also characterized at least in part by chronic inflammation; however, the variety of tissues they can reside in and effector molecules they're capable of interacting with may be one possible advantage of having both dispensable and foreign DNA [32]. Extra-oral *S. mutans* infections have been implicated in the etiology or as a risk factor in systemic diseases such as bacteremia, infective endocarditis, atherosclerosis, stroke, and inflammatory bowel diseases.

### 1.6.1 Key virulence factors involved in extra-oral infections

As mentioned previously, the species *S. mutans* is further subdivided into serotypes based on the structure of specific extracellular polysaccharides, called the rhamnose glucose polysaccharides (RGP). Serotypes e, f, and k which are somewhat rare in the oral cavity, but more frequently detected in extra-oral sites [33, 34]. Evidences suggests that differences in the level of expression and structure of serotype polysaccharides may be a major contributor to their enhanced virulence, mainly through reduced phagocytosis which increases survivability in the blood [35, 36]. These rare serotypes also tend to have higher expression of collagen binding proteins, especially those encoded by the gene *cnm*, which can bind and initiate adherence to a variety of host tissues [35, 37]. Although other cellular components of *S. mutans* have been implicated in systemic diseases, those interactions are more specific to each and will be discussed later. The general hypothesis for establishment of extra-oral *S. mutans* infections is as follows: *S.*

*mutans* gains access to the blood and avoids phagocytosis long enough for its collagen binding protein (CBP) to interact with and begin adhesion to susceptible host tissues [38, 39].

### 1.6.2 Bacteremia

Almost all extra-oral infections of S. mutans begin with at least transient bacteremia. The concentration of oral bacteria in the blood spikes minutes after dental procedures and in some cases after brushing alone, although brushing rarely resulted in a bacterial load that reached the threshold concentration of $10^4$ CFU/ml for extra-oral infections to take place [40]. Administration of amoxicillin capsules before dental procedures greatly reduced the number of CFUs in the blood [40].While it may not be recommended to administer prophylactic antibiotics before every dental procedure, a patient's risk factor for IBD, cardiovascular diseases, or hemorrhagic stroke could likely be compelling enough to recommend a patient take antibiotics prior to dental procedures. Being at high risk for these diseases could be an indicator for the presence of tissue damage that the cnm encoded CBPs of virulent S. mutans strains tend to latch onto and exacerbate [35, 37]. Research on oral bacterial entry into the blood indicate it's much more common than anticipated and so is also resolved by the immune system uneventfully more often than we had anticipated. On the other hand, the need for preventative measures can be justified in cases where the patient condition puts them at risk.

Research in this area tends to focus on *S. mutans* longevity in blood because usually the bacteremia is either transient and uneventful for healthy individuals, or transient but subsequently life threatening for those with certain conditions or predispositions. Because *S. mutans* grows in the form of biofilms and often becomes encased by immune cells once colonization takes place, the efficacy of subsequent treatment is limited, placing an even greater need for early detection and/or routine preventative measures. Most treatments studied and utilized in the field after it's entered the blood stream aim to reduce survival time, which restricts their ability to make contact with an appropriate tissue and colonize. Several genes have been identified as reducing the

phagocytic rate of *S. mutans* in blood. For example, biofilm regulatory protein A, BrpA, was shown to dictate chain length, resulting in longer chain formation when mutated and a lower phagocytic rate [41].

### 1.6.3 Infective endocarditis and atherosclerosis

Infective endocarditis (IE) is characterized by persistent inflammation following formation of a vegetation that contains bacterial cells, in the form of a biofilm, platelets and, immune cells [42]. According to a large study on the diversity and distribution of microorganisms found in plaque samples from patients who had infective endocarditis, Streptococcus species were the most commonly found and *S. mutans* specifically was found in 15% of samples [36]. Sequencing of bacterial rRNA from within atherosclerotic plaques of coronary artery disease patients showed that 75% contained S. mutans rRNA [43, 44]. Atherosclerotic plaques also contain a variety of other species resembling environmental biofilms including in the sequence of colonization, for which *S. mutans* is an initial colonizer [45]. The formation of biofilms is important because they are much less susceptible to antibiotic treatments and host immune responses [42].

Mice injected with virulent strains of *S. mutans* had accelerated plaque accumulation and inflammatory cell invasion [46]. *S. mutans'* role in IE has been thoroughly studied and has implicated the CBPs and RGPS mentioned above as virulence factors as well as several others, involved in decreasing phagocytosis, attachment to host tissues, activation of platelet aggregation, and stimulation of the immune system. None of the bacterial components associated with these hallmarks are expressed by all members even within the same serotype, so there is considerable variability across strains, even non-virulent type strains of the same serotype are used as controls in many studies.

*Serotype polysaccharides*

Serotype polysaccharides generally are composed of a rhamnose backbone and glucose side chains, but serotype *k* strains lack glucose side chains completely [36].The prevalence of

non-serotype *c* strains in cardiac specimens from patients with IE is significantly higher than in healthy patients [47]. Although the evidence has not shown that serotypes e and f do not have clinically relevant differences in RGP structure as compared to serotype c, but rather they have alterations of other surface and secreted molecules that are hypothesized to contribute to their virulence in cardiovascular diseases [47]. Serotype k however has lower amounts of glucose in their side chains which is hypothesized to reduce their phagocytic rate [35].

The inflammation that characterizes endocarditis is brought on in part by the activity of TNF-alpha and IL-1beta, the production of which is mainly carried out by mononuclear phagocytes in response to bacterial cell surface components or secreted molecules [42]. Evidence suggests that RGPs bind to both the CD11b and CD14 receptors of monocytes and binding of CD14 induces expression of TNF-alpha, a major mediator of inflammation [48]. Other research has also shown that a variety of RGPs bind to platelets and activate them, leading to aggregation [49].

*Collagen binding protein*

Serotype *k* strains tend to be more virulent due to their increased resistance to phagocytosis provided by the diminished immunogenicity elicited by their altered RGPs. Serotype *k* strains show better adhesion to host cells and evidence indicates a higher level of overall of CBP expression in serotype *k* strains, although there is variability within all serotypes [34]. A number of *S. mutans* isolates from the oral cavity and extirpated heart valves were screened for their ability to adhere and invade human coronary artery endothelial cells, and only those that were capable of adherence and intracellular invasion of endothelial cells, expressed CBP, suggesting a considerable role of CBP in IE [50]. In a study using balloon angioplasty injury to create a pro-atherogenic mouse model, injection of a virulent strain isolated from the heart of an IE patient and known to express CBP, resulted in increased plaque formation and inflammatory cell recruitment [42]. Expression of CBP confers an elevated level of virulence as it provides a means

of attachment to host cells, intracellular invasion, and increased plaque formation due in part to localization of inflammatory cells.

*Glucosyltransferases*

Glucosyltransferases (GTFs) are surface or secreted proteins with an enzymatic domain which process sucrose into glucans. In the oral cavity, these glucans are used as a scaffold for adhesion via the glucan binding domain of GTFs [9]. However, sucrose is rare in the blood so adhesion via glucan binding is impeded. This environmental aspect of the blood also supports previous research suggesting the collagen binding protein, Cnm, is vital to endothelial cell attachment [37]. Both surface and secreted GTFs can stimulate endothelial cell production of inflammatory cytokines and chemokines, inducing mononuclear cell chemotaxis to the site and increased monocyte adhesion upon arrival, which is required for sustained inflammation [51]. The binding of GTFs with endothelial glycoproteins also stimulates production of interleukin-6 which has an autocrine effect on the monocytes, inducing them to also express adhesion molecules [52].

*Other bacterial components involved in platelet aggregation and immunomodulation*

*S. mutans* mutants with a defect in BrpA, not only created longer chains which inhibited phagocytosis, these mutants also strongly induced platelet aggregation [41]. The cell surface protein antigen C (PAc) is responsible for initial binding to the tooth surface, but in the bloodstream these surface structures induce platelet aggregation [53]. It's also important to note that strains lacking PAc and with reduced GTF expression had no platelet aggregating effects, suggesting they are the major contributors to platelet aggregation.

A recent study looking at the specific mechanism of *S. mutans* induced expression of cytokines by aortic endothelial cells, found that all 6 of the strains tested from various serotypes had increased levels of TLR2 and NOD2 mRNA [53, 54]. Five of the six strains tested also enhanced endothelial cell production of IL-6, IL-8, and monocyte chemoattractant protein 1

(MCP-1) indicating the ability of *S. mutans* to elicit a strong inflammatory cascade [54]. Unfortunately, the authors did not consider which specific bacterial structures were interacting with the endothelial receptors, only citing previous research mentioned above suggesting GTFs or serotype polysaccharides are the specific immunomodulating components.

### 1.6.4 Hemorrhagic stroke

Although *S. mutans* alone cannot cause a hemorrhagic stroke, certain strains in the blood localize at sites of endothelial damage by binding to stripped down collagen using CBPs which are a key factor in determining *S. mutans* virulence in patients with existing endothelial damage [37]. Elevated levels of Cnm-positive *S. mutans* in the oral cavity were found in individuals with deep cerebral microbleeds (CMB) as well as asymptomatic CMBs [33, 55]. The exposed collagen that the bacteria tend to localize on is usually bound with platelets to prevent further bleeding, but *S. mutans* localization does not completely occlude the damaged areas that likely continue to bleed [33]. Activation of MMP-9 was also enhanced in sites where *S. mutans* was localized and even injection of purified CBP alone aggravated damaged endothelial cells [33].

### 1.6.5 Irritable bowel disease

The inflammatory responses generated by *S. mutans* impacts other diseases that do not involve endothelial cells, but again where chronic inflammation is a major component of its pathophysiology. Some of the oral manifestations of irritable bowel disease include higher incidence and severity of periodontal and carious sites as well as increased salivary *S. mutans* concentrations [45, 56]. Researchers also observed that mice injected with strains isolated form stroke patients not only increased the likelihood of cerebral hemorrhages and microbleeds, but also induced intestinal inflammation [37]. These observations and those of oral manifestations of IBD in patients have led to a recent rise in interest in oral bacteria's role in IBD, with many oral microbes being implicated, including S. mutans. Although there are reports of an association

between Chron's disease and caries causing bacteria, research so far has only elucidated details of the relation between ulcerative colitis and oral bacteria [57].

*Ulcerative colitis*

After observing inflamed intestinal tissue in mice injected with virulent strains of *S. mutans*, the researchers investigated its role in enhancing inflammation of the gut using a mouse model with induced colitis and injected them with virulent strains of *S. mutans* [35]. Surprisingly, they found the infections localized to the liver instead of the intestine itself and in vitro analysis showed when these virulent strains were exposed to hepatocytes, increased levels of IFN-gamma were found as confirmed by both RT-PCR and histochemical analysis. Histological analysis of mice tissues also showed increased intestinal IFN-gamma, supporting their hypothesis that bacterial induced cytokine production in the liver may be the first step in the inflammatory process. Virulent strains of *S. mutans* and *S. sanguis* also had high adhesion to and invasion of hepatocytes, suggesting that intracellular invasion of S. mutans is not unique to endothelial cells [58]. Higher adhesion rates in hepatocytes were also associated with cnm-positive strains and they confirmed the induction of IFN-gamma expression.

Recent research has led to the discovery of many connections between the oral microbiome and diseases outside the oral cavity. These studies have pointed to a need for more preventative measures to be taken before dental work and are paving the way for more specific diagnostic tools that could determine the risk of a patient with bacteremia based on the presence of specific virulence factors. By combining the recent findings in this area, healthcare providers may eventually be able to choose treatment options more precisely based on patient predispositions and bacterial characteristics, that will both protect the patient and prevent unnecessary antibiotic use and healthcare costs.

## 1.7 Lateral flow assay overview

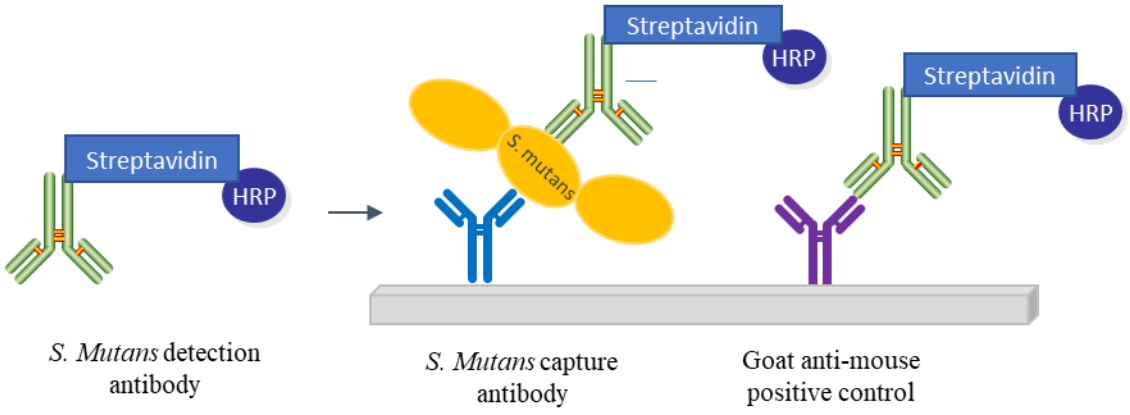


**Figure 1.** Full sandwich assay schematic for detection of S. mutans using Streptavidin-HRP conjugated antibodies for detection.

Lateral flow immunoassays (LFAs) rely on several common components such as a nitrocellulose membrane where capture antibodies are embedded onto the nitrocellulose first by the affinity nitrocellulose has for proteins through both electrostatic and hydrophobic interactions and by subsequent heat fixation [59]. A sample pad, which is usually composed of glass fiber, allows slow entry of sample fluids onto the membrane in order to prevent overflow and introduction of bubbles which impede flow. The sample is wicked through the membrane by the absorbent pad which is opposite the sample pad. In figure 1, the role of each component for detection of analyte as the absorbent pad wicks sample over the nitrocellulose is indicated. The capture antibody's affinity for the analyte will cause analyte accumulation over the spot when a sample containing the analyte is flowed over the strip. Before application to the test strip, samples were incubated to allow the detecting antibody to associate with streptavidin-HRP and for the detecting antibody complex to bind the bacteria. Control antibodies are also spotted on the strip and are usually specific to the detecting antibody only and ensures the assay was successful. For this assay the positive control spot was a goat anti-mouse (GAM) antibody that binds to any antibody produced in a mouse. Since all antibodies tested for use in the assay were of mouse origin, any chosen for the detection position, would bind regardless of the presence of bacteria.

Sample solutions contained detecting antibody conjugated to biotin, streptavidin-HRP (horse radish peroxidase) with or without bacteria. With the addition of substrate, the detection antibody associated HRP will produce a chemiluminescent or colorimetric signal, depending on the type of substrate chosen. When the detecting antibody is unconjugated, the addition of a secondary antibody that binds the detecting antibody and produces the signal is required.

## 1.8 Overall approach to the development of a LFA for detection of *Streptococcus mutans*

### 1.8.1 Antibody selection

The first objective was to select *S. mutans* specific antibodies. Although antibodies can be purchased ready-to-use, hybridoma cell lines offer a nearly limitless supply of monoclonal antibody, however the cells must be cultured and supernatant purified. Since they can be produced as needed, long-term storage stability was less of a concern. Hybridoma cell lines are identical populations of B cells, that produce and secrete a single antibody that binds to one specific region of an antigen, known as an epitope. The B cells are isolated from animals previously injected with the specific antigen/ pathogen of interest and then fused with tumor cells so that they can survive in vitro while still secreting antibody. The two hybridoma cell lines selected for this assay were suitable for use in clinical diagnostics and offered high specificity with no reactivity against any closely related species that also frequently reside in the oral cavity [60].

### 1.8.2 Biotin conjugation of detection antibody

To circumvent the need for a secondary antibody, a portion of both purified antibodies were conjugated to a signal-producing molecule like HRP. One of the more commonly used and simple methods for antibody conjugation is through biotinylation. Biotin binds very strongly to the protein streptavidin, and there are many commercial kits available for biotinylation of proteins and other biological molecules as well as ready to use strep-HRP conjugates. Both purified antibodies were biotinylated so that upon incubation with strep-HRP, antibody conjugates with signal-producing molecules associated will form and promote localization of signal producing molecules, in this case HRP, to the region of the test strip where analyte has accumulated over the capture antibody. Any unbound detecting antibody and associated HRP will flow with the fluid front to the absorbent pad.

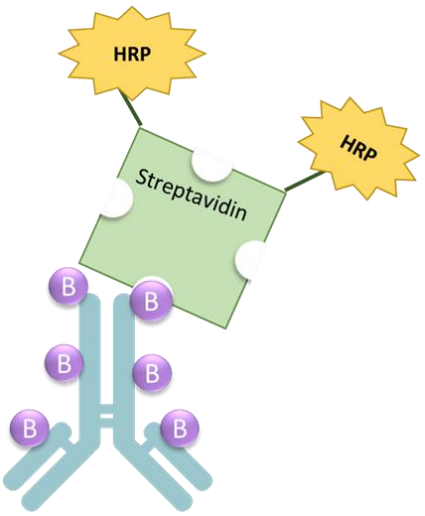


**Figure 2.** Diagram showing streptavidin-HRP attachment to biotinylated antibodies

### 1.8.3 *S. mutans* strain selection

The *S. mutans* strain ATCC 25175 is one of the most well-studied and is of serotype c, the most common serotype of *S. mutans* found in the mouth [61]. It also happens to be the strain to which each of the SWLA hybridoma lines was raised against; therefore, it served as the primary strain for assay development described in this thesis. However, dental caries will contain a mixture of the serotypes, that are also likely contributing to disease. Consequently, an additional strain of an undefined serotype was also used to test the antibody affinity and accuracy of the test through development.

## 1.9 Thesis overview

The impact caries and periodontitis have on quality life is sizable, globally pervasive and their role in the development and progression of systemic diseases also makes them potentially life-threatening. These factors indicate a need for a point of care diagnostic that detects oral pathogens like *S. mutans*. The ability to rapidly identify *S. mutans* in the oral cavity gives insight not only into the patient's dental caries status and severity, but it can also give healthcare providers a better idea of caries risk during periodontal disease. The goal of this research was to develop a lateral flow assay able to detect *S. mutans* in saliva samples, in order to diagnose dental caries. In the following sections the methods and results are used to obtain antibody from hybridoma supernatant and screening of those antibodies against the two strains of bacteria is outlined. Initial results of the full sandwich LFA and steps to optimize its detection are described. Lastly, a dose response curve was created to determine analytical performance of the assay by testing a range of *S. mutans* concentrations in human pooled saliva.

# 2 MATERIALS AND METHODS

## 2.1 Reagents and Materials

Table 1 lists key cell lines and media reagents that were used in this work and their product numbers. All cell lines, both hybridoma and bacterial stocks, were sourced directly from American Type Culture Collection (ATCC, Manassas, VA). Standard untreated 96-well plates, catalog number 266120, were obtained from Thermo Fisher Scientific (Waltham, MA). Buffer reagents and chemicals were soured from Sigma Aldrich (St. Louis, MO), unless otherwise noted. PBS buffer was made from BupH

Modified Dulbecco's phosphate buffered saline packs, sourced from VWR (Product number 28374) and contained: 0.008M Sodium Phosphate, 0.002M Potassium Phosphate, 0.14M Sodium Chloride, 0.0027M Potassium Chloride, pH 7.4. The following buffers were used in antibody purification: Phosphate buffer pH 7.5, Tris-HCl pH 9.0, and 0.1M Gly-HCl pH 2.7. Substrate used in all assays was Supersignal west pico chemiluminescent substrate product number (product number 34080). Nitrocellulose embranes used in all assays were Millipore HiFlow Plus HF75 (Product number HF07504X).

**Table 1**. Table listing important reagents and product numbers used in this work.

| **Cell line**/ Growth media | **manufacturer** | **Sourced from** | **item number** |
|---|---|---|---|
| *S. mutans* hybridoma: SWLA-1 | ATCC | direct | HB-12559 |
| *S. mutans* hybridoma: SWLA-2 | ATCC | direct | HB-12560 |
| *S. mutans* hybridoma: SWLA-3 | ATCC | direct | HB-12558 |
| S. mutans strain 25175 | ATCC | direct | |
| S. mutans strain 35668 | ATCC | direct | |
| Bacto brain heart infusion powder | BD | vwr | 237500 |
| agar | Thermoscientific | vwr | BP1423 |
| HL-1 completely defined serum free culture medium | lonza walkersville inc | vwr | 344017 |
| BioWhittaker* HL-1 Supplement (100x) | lonza walkersville inc | vwr | 77227 |

## 2.2 Bacterial culture and characterization

### 2.2.1 General growth protocol

Two *S. mutans* strains (#25175 and #35668) were obtained from American Type Culture Collection (ATCC, Manassas, VA). Upon receipt, each culture was expanded by streaking the frozen stock onto a Brain Heart Infusion (BHI) agar plate that was incubated at 37˚C with 5% $CO_2$ for 72 – 96 hrs. When individual colonies on each plate were apparent, an inoculating loop

was used to collect the colony and transfer it to 4.5 ml sterile liquid BHI broth in a 10 ml glass test tube. Initial liquid cultures were incubated at 37°C with 5% $CO_2$ for 24 hours without shaking. After incubation sterile glycerol was added directly to the broth cultures to make 50% glycerol stocks that were stored at -80°C. To start bacterial cultures from frozen stocks stored at -80°C, a heat sterilized inoculating loop was used to scrape the top of the contents of the frozen vial and then streaked onto a brain heart infusion agar plate. The plate was then placed in a 37°C incubator with 5% $CO_2$ and incubated for 24 hours. All bacteria used for testing in LFA were from liquid cultures. After colony formation on agar was apparent, one colony was scraped from the agar using a heat sterilized inoculating loop and placed in a 10ml test tube containing 4.5 ml of BHI broth. Inoculated broth tubes were then incubated again at 37°C with 5% $CO_2$ for 24 hours without shaking.

### 2.2.2 Staining and imaging

First, to homogenize the liquid culture, the test tubes were vortexed for a few seconds. Then an inoculating loop was placed in the test tube and once a thin film across the loop was seen, it was spread in a small area in the center of a glass microscope slide. To heat fix the bacteria the slide was waved over the Bunsen burner flame 3 times. One drop of 0.01% crystal violet was placed over the spot of heat fixed bacteria and incubated for 1 minutes. The crystal violet was then rinsed with DI water until runoff was clear. Gram's iodine was then applied to the slide and incubated for another minute. Iodine was rinsed with DI water and then decolorized by flooding with 70% ethanol for 10 seconds. Excess ethanol was rinsed with DI water before applying safranin counter stain. Safranin was rinsed with DI water and the slide was dried with bibulous paper. Slides were viewed with Leica model CME microscope (model #1349521X) under 100x magnification, numerical aperture 1.25 using the oil immersion lens.

### 2.2.3 Growth curve

In a 96-well plate sourced from VWR (product number 266120), 200 µl of sterile BHI broth was placed in each of the 3 negative control wells. All other wells contained 190 µl of sterile BHI broth with 10 µl of broth from an overnight *S. mutans* culture added to each. Once the plate was loaded with broth and overnight culture, it was placed in a PowerWave XS Biotek plate reader and incubated for 72 hours with shaking at 37°C. Optical density (OD) readings at 600 nm wavelength were recorded every hour to establish the bacterial growth rate.

### 2.2.4 Standard curve

A liquid culture at an OD of 1 was diluted to ODs of 0.9, 0.8, 0.7, 0.6, 0.5, 0.4, 0.3, 0.2, and 0.1. For each OD value (1.0-0.1) a 1:10 serial dilution was carried out to a dilution factor of $10^{-7}$. Solutions with dilution factors of $10^{-4}$ -$10^{-7}$ were plated on agar plates using 100 µl of the diluted culture for each plate. The 100 µl aliquots were spread over the agar with a heat sterilized glass spreader. Agar plates were incubated 1-2 days at 37°C with 5% $CO_2$ until colonies were clearly visible. The number of colonies on each plate was counted and only those between 30 and 300 were used to create the standard curve.

## 2.3 Cell culture

All SWLA cell lines were cultured in HL-1 completely defined serum free media with 1X HL-1 media supplement, a fetal bovine serum (FBS) substitute, as well as 4mM L-glutamine. Upon receipt of hybridoma cell lines from ATCC, each cell line was expanded to create frozen stocks. To begin expansion, cryovials were removed from -180°C storage and immediately warmed in the water bath until completely thawed. After spraying with 70% ethanol, they were placed under the hood and allowed to dry. Two ml of complete pre-warmed complete media was added to a 15ml conical tube and the contents of the thawed cryovial was added to the same tube. Cells were spun down at 1,000 xg for five minutes, then the supernatant was removed and the

pellet resuspended in two ml of pre-warmed media. 10 µl of the resuspended cell solution was used to count the cells on a hemocytometer and the volume of media cells were resuspended in, was adjusted to achieve a seeding density of $5x10^5$ cells/ml. Cells were cultured in vented CELLSTAR T75 flasks sourced from VWR (Product number 658175) and checked daily until they had doubled at which point they were split, as described below.

To split the culture, the flasks were scraped lightly with a falcon cell scraper, sourced from VWR, using a side-to-side motion, then the contents of the flask were removed and transferred to a conical tube to be spun down at 1,000 xg for five minutes. The supernatant was removed and stored at 4°C for later purification. The cell pellet was resuspened in two to four ml counted and media volume adjusted to achieve a seeding density of $5x10^5$ cells/ ml. The cultures were checked daily and split as needed. Cultures were checked and split as needed until growth reached the exponential phase at which point, cells were pelleted by centrifugation at 1,000 xg for 5 minutes. Cell pellets were resuspended in fresh culture media containing 10% DMSO, which was aliquoted at 1ml into cryovials, and stored at -180°C.

Cultures were initiated from frozen stocks for antibody purification using the same methods described above. Instead of creating frozen stocks, once the total media volume was above 60ml they were allowed to die off over the course of about a week before harvesting the culture supernatant and proceeding to purification.

## 2.4 Antibody purification

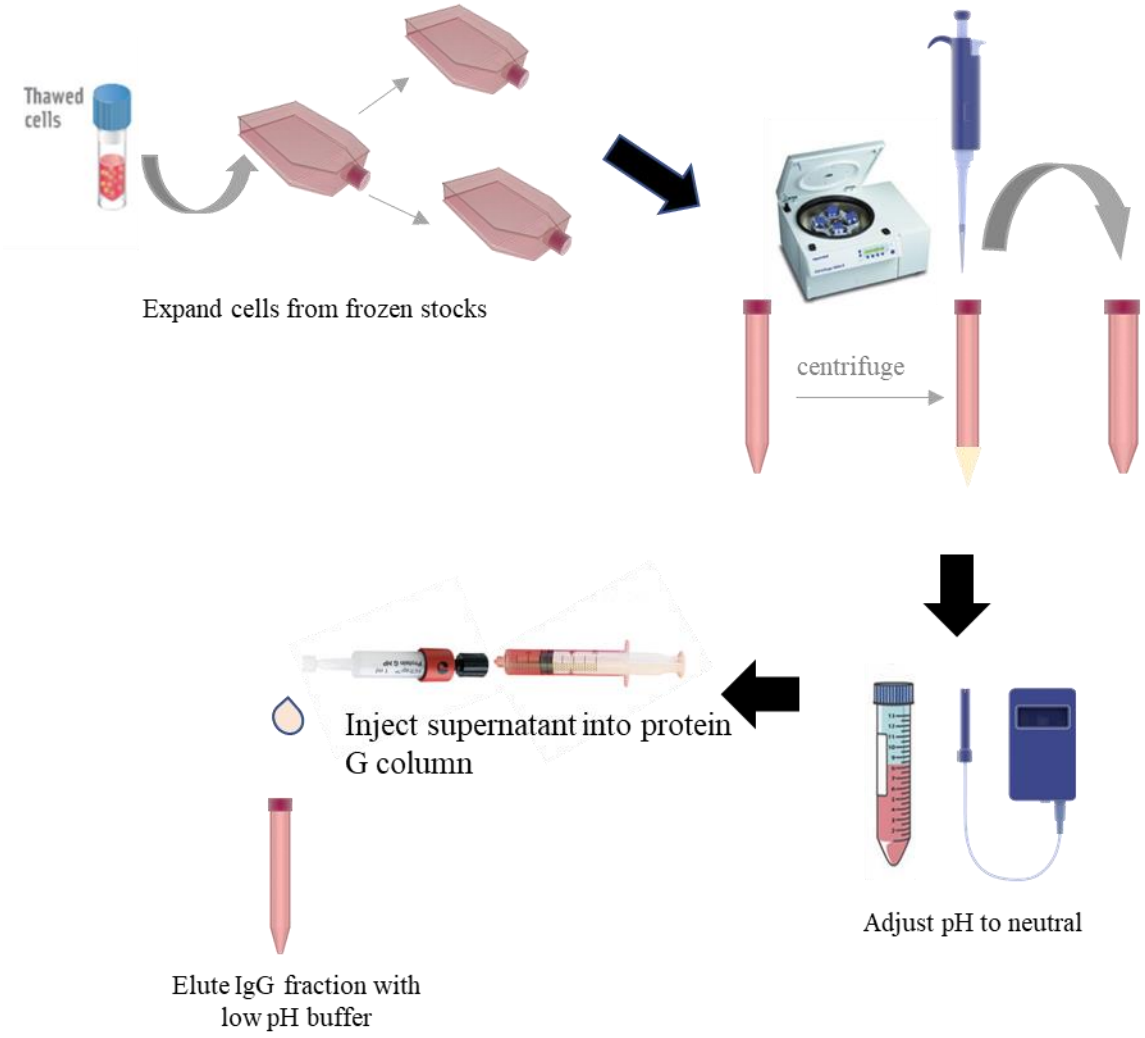


**Figure 3.** General schematic of antibody purification process, from cell culture to affinity chromatography

Figure 3 depicts the steps of antibody production starting from expanding hybridoma cultures, then isolating supernatant from the cells, adjusting the pH to neutral, and after application onto the column, eluting antibodies with a low pH buffer. Protein G is a pH dependent affinity chromatography media that binds IgG at near neutral pH, but under acidic conditions the protein G-IgG interaction is not favored. The column pre-equilibration steps use neutral buffers to promote IgG binding, the sample is also prepped prior to column infusion to be at a neutral pH and after washing away unwanted cellular proteins, the antibody can be eluted.

Cell cultures were removed from their flasks, placed in conical tubes and spun down at 2,500 xg for 5 minutes to remove cells. The supernatant was removed, and the pH adjusted to 7 by adding 2-4N NaOH as needed. The supernatant was then filtered through a 0.2 µm PES (polyethersulfone) membrane to remove any remaining cellular debris. Affinity chromatography was carried out using a HiTrap protein G HP column sourced from GE life sciences (Pittsburgh, PA) with product number17-0405-01. Instructions from manufacturer protocol for syringe pump set up were followed. Pre-equilibration of the column was completed by infusing 10 column volumes of Phosphate buffer, pH 7.5, and a flow rate of 1 ml/min for 1 ml columns and 5 ml/ min for 5 ml columns. After equilibration the sample was infused at a rate of 0.2-0.4 ml per minute. Unwanted cellular proteins were washed away with the infusion of 8-10 column volumes of phosphate buffer at 1 ml/min or 5 ml/min depending on column size. Antibody was eluted with 5 column volumes of 0.1M Gly-HCl pH 2.7 at an infusion rate of 1 or 5 ml per minute. Eluate collection tubes contained 200 µl of Tris-HCl pH 9.0 for every 1 ml of eluate.

Protein concentrations for each elution fraction were determined by taking absorbance readings at 280 nm wavelength on a Synergy H1 hybrid reader biotek. The antibodies elute at much more dilute concentrations than are needed for storage and use in LFAs, so elution fractions with protein, were concentrated with Amicon 30K centrifugal filter units (sourced from VWR) by spinning at 14,000x g for 10-15 minutes. 100-200 µl of PBS was added to concentrate volume remaining on the filter column, and spun again at the same speed and time to replace the elution buffer with PBS. Purified antibodies were stored at 4°C in 10 µl aliquots at concentrations between 0.8- 2.0 mg/ml.

## 2.5 Antibody conjugation

Antibody conjugation was done using EZ-Link™ NHS-LC-Biotin kit sourced from VWR (CAS 72040-63-2) and the Manufacturer protocol for conjugation to proteins was followed. A 20 mM

biotin solution in anhydrous DMSO was made by measuring the appropriate weight of biotin powder, provided in the kit. The appropriate volume of the biotin solution was added to the antibody solution in a volume that achieved a 12 or 20mM excess of biotin and allowed to incubate on ice for two hours. Excess biotin was removed by adding 100-200 µl PBS to antibody biotin solution and then spinning down at 14,000xg for five minutes in amicon 30k molecular weight cut-off columns.

## 2.6 Half-sandwich assay

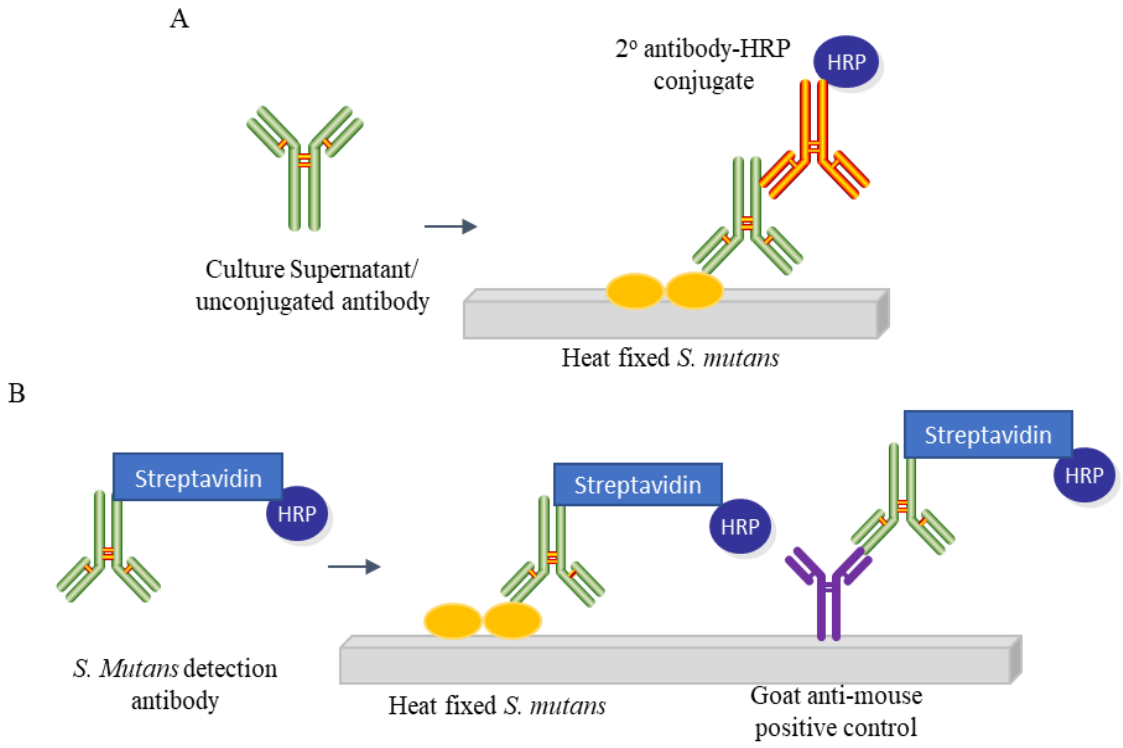


**Figure 4.** Half sandwich assay schematic used for initial determination of activity against antigen. (A) Set up for half sandwich assay used for testing culture supernatant or unconjugated purified antibodies (B) Set up for half sandwich assay used for testing biotin conjugated antibodies.

Half sandwich assays were used as a preliminary step to determine antibody affinity for antigen while eliminating many of the complicating factors that can affect the outcome of a full sandwich assay. Figure 4 shows a schematic of the half sandwich assay which also uses a lateral

flow test strip with antigen fixed directly to the surface and the antibody of interest is then flowed over the antigen spots where it should become immobilized. For unconjugated antibodies, a subsequent solution containing a secondary antibody conjugated to HRP was flowed.

### 2.6.1 Membrane preparation

Nitrocellulose adhesive cards were cut to a width of 4mm and the adhesive portion, where the sample pad would usually go, was cut off. Absorbent pads were also cut to a width of 4 mm and a height of 55 mm. Bacterial cultures were spun down at 1,000 xg for 5 minutes, supernatant removed and resuspended/diluted in PBS to desired optical density (OD), usually 0.5 or 1.0. 0.5 µl spots of bacterial suspensions of known OD were hand spotted onto the nitrocellulose using a pipette. Once all the spots were dispensed onto the membrane it was placed into a 37°C incubator for 1 hour, in order to fix them to the nitrocellulose. The membranes were then blocked with BSA by pipetting 50 µl of a 1% BSA-PBS solution onto the membrane. The BSA solution incubated on the membrane for 5 minutes before briefly submerging them in a 0.05% PBST solution and wicking excess liquid with a kim wipe. The strips were then placed in the incubator at 37°C for 35 minutes. The absorbent pad was attached to the remaining adhesive portion of the nitrocellulose strip with a 2 mm overlap onto the nitrocellulose.

### 2.6.2 Running the assay

Half sandwich and full sandwich assays were carried out using the dipstick method. This method involved test strips with an absorbent pad attached at the top and for full sandwich assays a sample pad also attached at the base. Assembled test strips were placed in an upright position, usually within a solution reservoir or a 96 well-plate, with the sample pad on the bottom placed in the sample or wash solution.

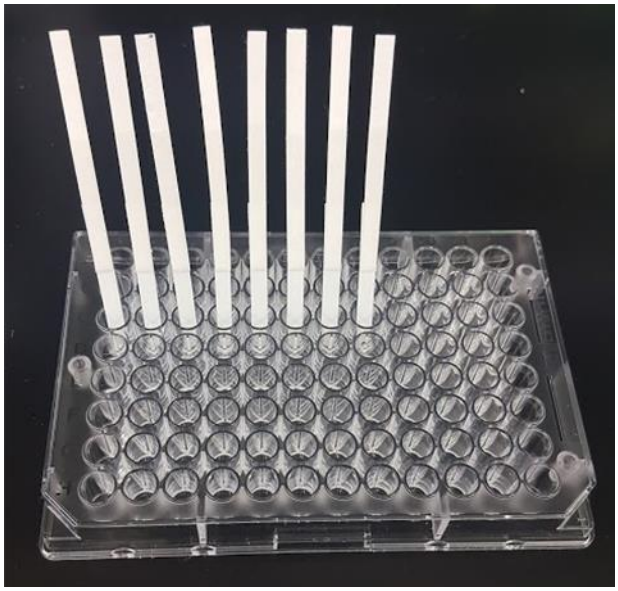

**Figure 5.** Example of dipstick assay format

Several solutions were loaded into the wells of a 96-well plate in 30µl aliquots. The composition and order of those solutions were dependent on whether the antibody to be screened was conjugated or unconjugated, and are listed for each below. After allowing each solution within the 96-well plate to flow completely, the membranes were disassembled and washed by submerging in 0.05% tween20-PBS solution for 30 seconds and repeated for a total of 4 washes. 50 µl of substrate was then pipetted onto each membrane directly and incubated in the dark for 2 minutes. Before imaging, excess substrate was removed with a kim wipe. A series of images were taken using GeneGnome 5 imager model No. 75000 and accompanying Genesys software version 1.5.7.0. Images were taken with 60 second exposures, 2x2 binning (1.25 MP), and only the $5^{th}$ image was used.

**Table 2.** Order of Solutions used for half sandwich assays (A) Buffers/ reagents used in each step of the half sandwich assay for verification of biotin conjugated antibodies. (B) Buffers/ reagents used in each step of the half sandwich assay for verification of unconjugated antibodies.

A

| Biotin conjugated | | |
|---|---|---|
| Order | concentration/dilution | Buffer |
| 1 | 10µg/ml antibody, 1-2µg/ml streptavadin-HRP | 1% BSA in PBS with 0.05% tween20 |
| 2 | wash | PBS with 0.05% tween20 |
| 3 | wash | PBS with 0.05% tween20 |

B

| Unconjugated | | |
|---|---|---|
| Order | concentration/dilution | Buffer |
| 1 | 10µg/ml antibody | 1% BSA in PBS with 0.05% tween20 |
| 2 | wash | PBS with 0.05% tween20 |
| 3 | 1:1,000 HRP conjugated Goat ant-mouse (2° antibody) | 1% BSA in PBS with 0.05% tween20 |
| 4 | wash | PBS with 0.05% tween20 |
| 5 | wash | PBS with 0.05% tween20 |

## 2.7 Full sandwich assay

### 2.7.1 Membrane preparation

Nitrocellulose membrane cards were cut to a width of 6.5mm. Cellulose absorbent pads were cut to dimensions of 30 mm x 18 mm. The glass fiber sample pad was cut to 6.5 mm wide and 15 mm long. Antibody spots were hand spotted with a pipette onto the cut nitrocellulose strips 3-4 mm below the adhesive where the absorbent pad was to be attached. Before spotting, the antibody was first diluted to the desired concentration in PBS. For hand spotting GAM was diluted to 0.1 mg/ml and SWLA-1 stock was already at0.8 mg/ml, then 0.5 µl of the solution was pipetted onto the membrane. Assays run for the dose response used test strips that were spotted

using a custom built automated aspiration and dispensing system (RQS spotter, Paratus Diagnostics, San Marcos, TX) which dispenses 30 nl droplets of antibody at a concentration of 0.1 mg/ml for GAM (3 ng total protein) and 2 mg/ml for SWLA-1 (60 ng total protein). Once all the spots were dispensed/ hand spotted onto the membrane they were placed in a 37°C incubator for 1 hour to fix the protein to the nitrocellulose.

Nitrocellulose is ideal for LFAs because of its ability to bind protein, so capture antibodies when spotted already have a natural affinity for the membrane: however, during the assay detection antibodies need to flow through the membrane, without prolonged interaction with the membrane potentially interfering with antibody-antigen interaction, for the assay to work properly. Blocking the membranes with a protein solution like BSA, reduces non-specific binding.

The membranes were blocked with BSA by pipetting 100 µl of a 1% BSA-PBS solution directly onto them. The BSA solution incubated on the membranes for 5 minutes before briefly submerging them in a 0.05% PBST solution and wicking excess liquid with a kim wipe. The strips were then placed in the incubator at 37°C for 35 minutes. The absorbent pad was attached to the remaining adhesive portion of the nitrocellulose strip with a 2mm overlap onto the nitrocellulose. The sample pad was applied to the other end of the strip with the same 2mm overlap onto the nitrocellulose. Sample pads were left untreated for all experiments unless otherwise stated. Treatment of sample pads was done by submerging pre-cut glass fiber into 1% tween -PBST solution for 1 hour, then blotting excess liquid with a kim wipe and drying at 37°C for 35 minutes.

### 2.7.2 Running the assay

To prepare the bacteria before adding to the sample, 1 ml of culture was spun down at 1,000 xg for 5 minutes. The pellet was resuspended in PBS and diluted to an appropriate OD reading at 600 nm wavelength. The detection antibody and Streptavidin-HRP were also diluted in

the same PBS buffer and all were combined in the sample solution with the total volume raised to 100 µl by adding the sample buffer, PBS as needed. The final concentration of detection antibody, biotinylated SWLA-3, was 500 ng/ml and the final Streptavidin-HRP concentration was 1 µg/ml. Assays run for the dose response also used PBS to resuspend and dilute the bacterial pellet, but all other components (sample buffer, detection antibodies and strep-HRP stocks) were in 2.5x diluted frozen pooled saliva. Frozen pooled saliva was diluted with 0.01% tween 20 in PBS. All other antibody/HRP concentrations and sample volumes were identical for the dose response as they were in initial testing and optimization.

The 100 µl sample solution flowed first, then a 250 µl PBS or PBS with0.05% tween 20 wash solution followed to remove any unbound antibody or HRP. The strips were then disassembled, and 100 µl of substrate pipetted directly onto the membrane. After a two-minute incubation in the dark, they were imaged for 5 minutes using a GeneGnome imager with 60 second exposures, only using the last image collected.

## 2.8 Image analysis

To assess analytical performance of the assay, ImageJ was used to determine signal intensity relative to the average background signal or "noise". Images were first converted to an 8-bit grey scale format and manually cropped to contain only the reaction zone. Threshold was adjusted so that positive control spots could be resolved from the background, with an area ranging from 25-40 pixels. After setting the threshold, particles with a size of 5-∞ and a circularity between 0.0 and 1.0 were analyzed. The intensity of the particle containing the *S. mutans* signal was then measured. When no signal was present for *S. mutans*, the size of the ROI measured for "signal" intensity was between 25-40 pixels and located over the same area the signal would've been expected. Average background intensity was measured at one random ROI with an area of about 1,000 and

repeated for each strip. The signal-to-background ratio was calculated by dividing spot intensity by the average overall background intensity.

## 2.9 Determination of LOD and LOQ

Limit of detection (LOD) is defined as the lowest analyte concentration that can be consistently differentiated from the average blank sample. Although some older methods only measure the signal from blank samples and extrapolate the LOD by adding at least one standard deviation to the mean of the blank, it is more accurate to also include data from tests with known amounts of analyte as well [62]. This combined approach is recommended by the clinical laboratory science institute which sets standards for testing of diagnostics [63]. The LOQ or limit of quantitation is the lowest analyte concentration that can be reliably differentiated from the LOB. The reliability of this value is based on preset goals, usually the lowest concentration with a %CV of 20 or less [64]. These standards may be met at the LOD, but are usually met at an analyte concentration higher than the LOD.

Assuming a normal or Gaussian distribution of values about one data point, (for one analyte or blank concentration) the equation below can be used to calculate the LOB and LOD:

LOB = Mean of the blank + (St.Dev. x 1.645)

LOD = mean of the blank + ($St.Dev._{[low\ analyte]}$ x 1.645)

These equations account for 95% of the variation that may occur at the LOB or LOD.

# 3 RESULTS AND DISCUSSION

## 3.1 Characterization of *S. mutans* strains

The morphology seen in the gram stain image of *S. mutans* ATCC strain 25175 is characteristic of the species, which has rounded, or coccus shaped cells linked together in chains (Fig. 6A). The purple coloring that resulted from the staining procedure is consistent with the fact that decolorizing with ethanol does not easily remove crystal violet from the thick peptidoglycan layer of gram positive cells. The morphology and color after gram staining for ATCC strain 35668 was also consistent with gram positives in general and the species specifically (Fig. 7A). However, strain 35668 tended to form chains of only two to three cells, while strain 25175 has many chains comprised of five or more cells.

Standard curves were created to determine the density of bacteria in solution by reading optical density (OD) values on a spectrophotometer. The equation for the line was used to determine bacterial concentration at a specific OD, since X is optical density and Y is CFUs/ml (colony forming units).

The maximum optical density seen on the growth curve for strain 25175 was around 0.7 and was achieved at the end of the exponential phase, which was about ten hours after the initial inoculation (Fig. 6C). Thereafter, the cells entered log phase and remained in a non-replicative state for the remainder of the 72-hour culturing time. The increase in optical density seen after about 50 hours would not usually be visible since most growth curves are only for a 48-hour incubation period. Although it was unusual, this could be explained by color changes in media or a small subpopulation of cells stills replicating while most of the culture is no longer replicating or dying.

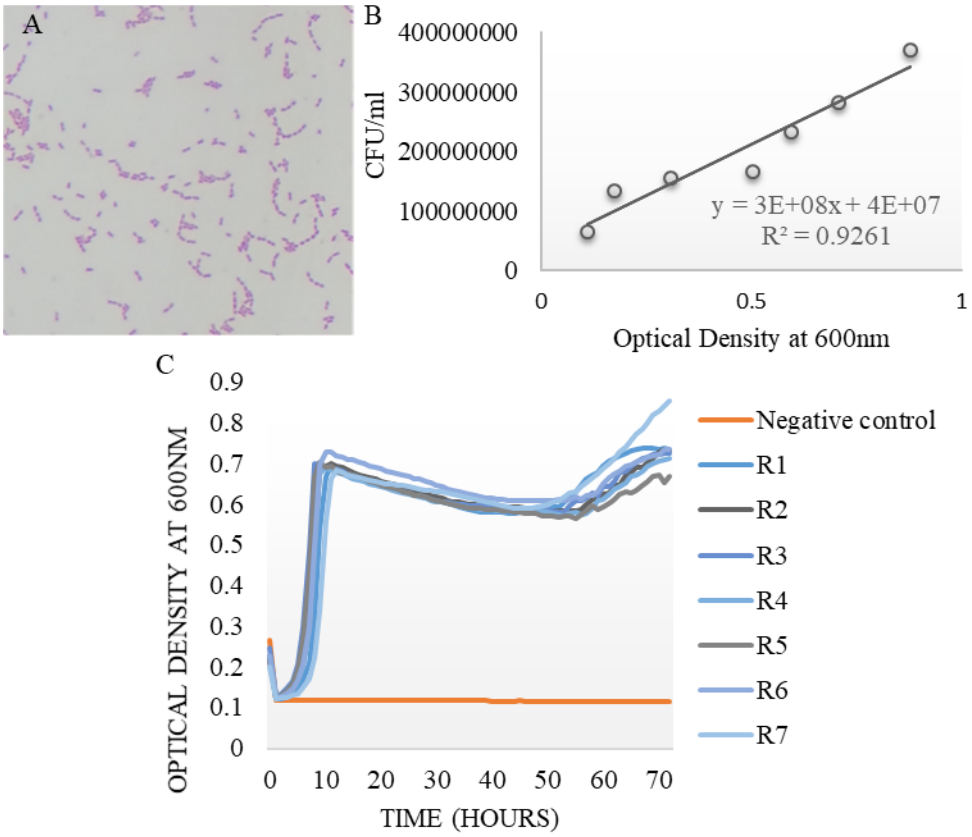


**Figure 6.** Characterization of *S. mutans* Strain 25175. (A) Brightfield image of gram stained *S. mutans* allowing visualization of cocci chains and clustering. 100x oil immersion objective, with numerical aperture of 1.25 (B) Standard curve showing optical density at 600nm as it relates to CFUs/ml (C) Optical density of broth culture at 600 nm over a 72 hour period. R1-R7 represent replicates 1-7.

The 72-hour growth curve produced for strain 35668 also had a lag phase that lasted for about five hours, then log phase continued for the next five to six hours and peaked at an OD around 0.7 (Fig. 7C). There was some variability among the replicates in the maximum OD reached at the end of their log phase, but all reached a similar OD in stationary phase. The Growth curves were used to determine the length of time to culture the bacteria before use in an assay. To reach the desired OD and ensure most cells were still alive and replicating, they were cultured overnight, or up to 24 hours ahead of time.

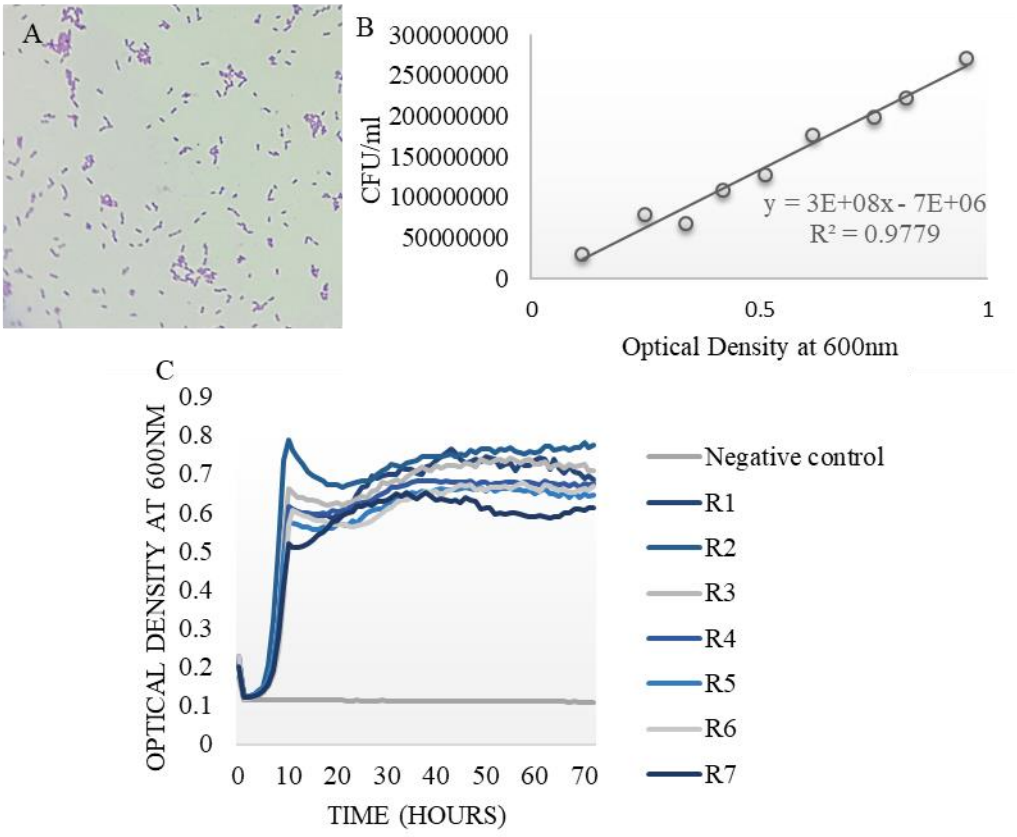


**Figure 7.** Characterization of *S. mutans* strain 35668 (A) Brightfield image of gram stained *S. mutans* allowing visualization of cocci chains and clustering. 100x oil immersion objective, with numerical aperture of 1.25 (B)Standard curve indicating Optical density at 600nm as it relates to CFUs/ml (C) Optical density of culture broth at 600nm over a 72 hour period. R1-R7 represents replicates 1-7.

## 3.2 Purification of antibodies from cell culture supernatant

SWLA-3 purification data listed in Table 3B, shows no consistent IgG yield even when length of culturing time is taken into consideration. Attempts to purify supernatant from SWLA-2 cultures were not successful and could not be included in the data listed in the table because the A280 readings were too low to be used as a reliable estimate of antibody concentration. Cumulative data form SWLA-1 purifications (Fig. 3A), indicates that antibody yield was consistently around 1.5 µg IgG for each milliliter of supernatant purified. The data for SWLA-1 purifications also does not indicate that the length of culturing time has a significant impact on

yield when considered separately from total volume. Although there is variability in antibody yield among individual purifications, optimization of this protocol was not needed since these purifications produced the IgG needed to complete the research.

**Table 3.** Cumulative antibody purification data from hybridoma supernatants by protein G affinity chromatography. (A) IgG yields from supernatants harvested from SWLA-1 cell lines. (B) IgG yields from supernatants harvested from SWLA-3 cell lines.

A

| SWLA-1 | | | |
|---|---|---|---|
| Volume supernatant | length of culture | Antibody yield | µg/ml purified |
| 60ml | 13 days | 88ug | 1.5 |
| 84ml | 16 days | 150ug | 1.8 |
| 125ml | 11 days | 221ug | 1.8 |

B

| SWLA-3 | | | |
|---|---|---|---|
| Volume supernatant | length of culture | Antibody yield | µg/ml purified |
| 58ml | 13 days | 151ug | 1.6 |
| 60ml | 14 days | 517ug | 8.6 |
| 60ml | 10 days | 288ug | 4.8 |

### 3.3 Screening of purified antibodies with half sandwich assay

In Figure 8B large bright signals were present over all GAM spots after flowing SWLA-3 with strep-HRP, indicating that biotinylation of the antibody resulted in a functionally conjugated protein. Two round signals below the GAM signal were present in decreasing intensity and these spots correspond to decreasing concentrations of *S. mutans* 25175 heat-fixed to the membrane (Fig. 8B). The resulting images collected after flowing SWLA-1 in a half sandwich assays, shows two equally bright spots at the top of the strip for every SWLA-1 concentration tested and a lack of any signal production on

strips with only secondary antibody flowed (Fig. 3D). The two antibody concentrations tested in both SWLA-1 and 3 half sandwich assays, resulted in the same level of signal strength (Fig 3B and 3D). Signal intensity produced in SWLA-1 half sandwich assays was comparatively higher than that seen for SWLA-3. Results from flowing SWLA-2 culture supernatant in the half sandwich indicates SWLA-2 antibodies recognize strain 25175, indicated by the two circular spots at the top of Fig. 8E.

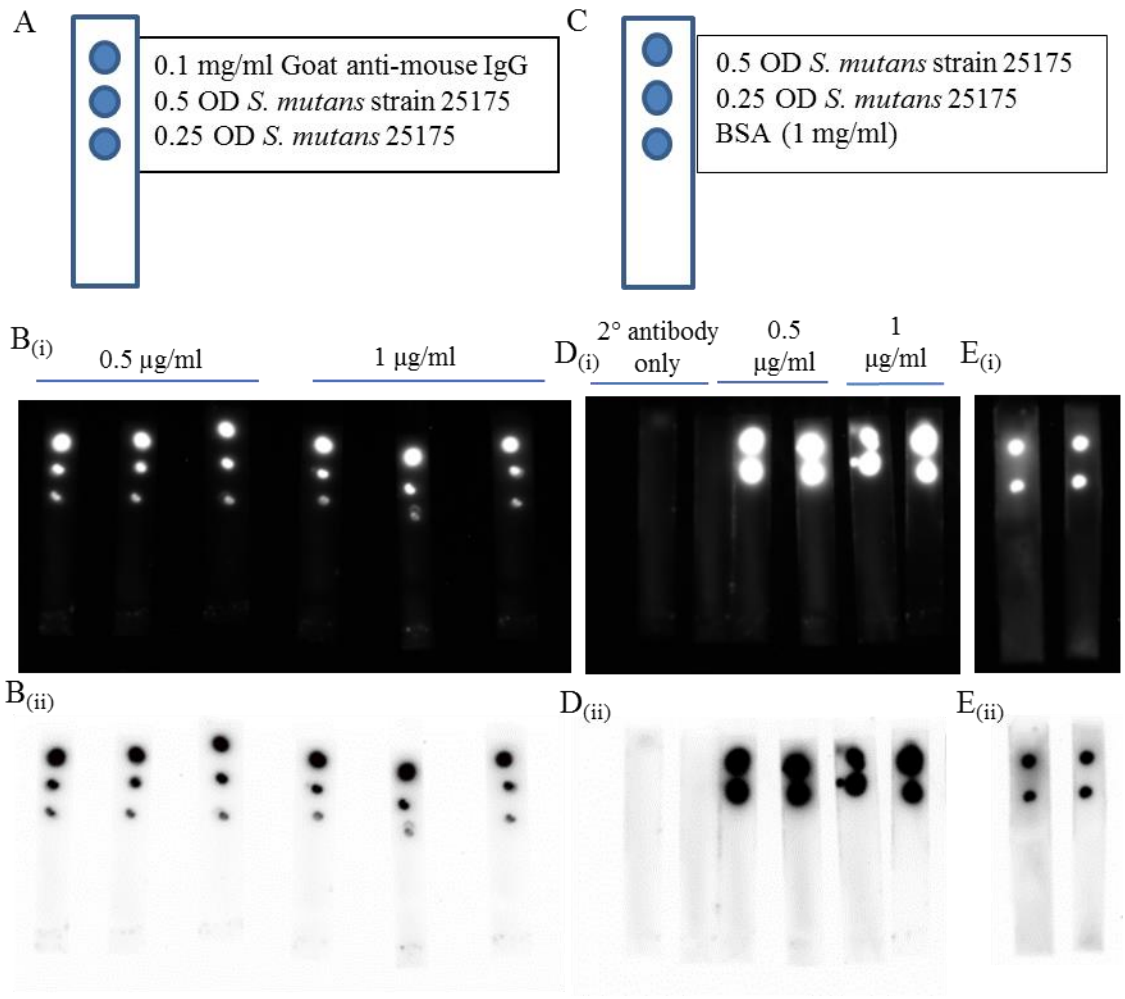


**Figure 8.** Half sandwich assay to determine preliminary antibody activity against strain 25175. (A) Layout of heat-fixed spots on nitrocellulose strip (B) Resulting images after flowing 0.5 and 1 µg/ml biotinylated SWLA-3 and streptavidin-HRP. 60 second exposure (C) Layout of heat-fixed spots on nitrocellulose strip for images in D and E (D) Resulting images after flowing secondary HRP conjugated antibody with or without unconjugated purified SWLA-1 at 0.5 µg/ml and 1 µg/ml. 60 second exposure. (E) Resulting images after flowing 1:1 diluted SWLA-2 supernatant.

All SWLA antibodies were active against strain 25175. SWLA-1 and SWLA-3 antibodies were affinity purified and in the case of SWLA-3, biotin conjugated, suggesting purification/ conjugation did not lower their binding affinity. Testing unconjugated antibodies requires a secondary antibody for signal production, and although they have a higher potential for cross-reactivity than most antibodies, no signal was produced with secondary antibody alone, ruling out cross-reactivity with *S. mutans* whole cells. Signal intensity produced in SWLA-1 half sandwich assays was comparatively higher than that seen for SWLA-3.

Results from the half sandwich assay used to screen antibodies against strain 35668, shown in Figure 9, display three circular signal spots at the top of the test strips used to screen SWLA-1 and -2 antibodies. Test strips used to screen SWLA-3 had only a GAM signal at the top (Fig. 9). Only SWLA-1 and 2 antibodies recognize this strain,

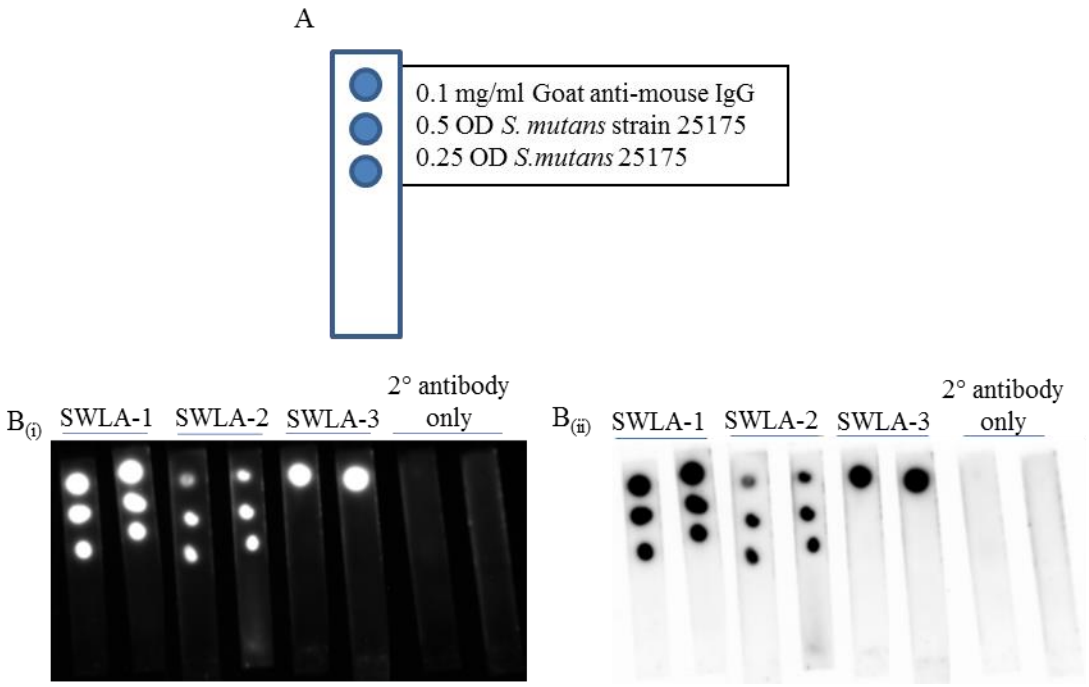


**Figure 9.** Half sandwich assay to determine preliminary antibody activity against strain 35668. (A) Layout of heat-fixed spots on nitrocellulose strip (B) Resulting images after flowing 10 µg/ml SWLA-1, 1:1 diluted SWLA-2 culture supernatant, and 10 µg/ml SWLA-3. 60 second exposure

while SWLA-3 does not. Although SWLA-1 and 2 antibodies could potentially make up a matched pair able to recognize surface features shared across multiple strains of *S. mutans*, attempts to purify SWLA-2 supernatant were not successful, so it was not possible to include this as a component of the full capture sandwich assay.

The lowest concentration tested for SWLA-3 (500 ng/ml) in the half sandwich assay was used in the full sandwich assay, while the highest concentration stock of SWLA-1 (0.8 mg/ml) was used in a full sandwich assay, which tested a range of bacterial concentrations (Strain 25175).

### 3.4 *S. mutans* full sandwich assay and initial dose response curve

Only one bright round signal was produced at the GAM spot on test strips flowed with a bacterial concentration of $1x10^4$ CFUs/ml or lower (Fig. 10B). The GAM signal remains constant at all other concentrations of bacteria tested. A half-moon shaped signal was present at concentrations at and above $1x10^6$ CFUs/ml, where the intensity and size of the signal produced progressively increased with the bacterial concentration. Faint signals are present at $1x10^5$ CFUs/ml, which is lower than the minimum concentration that should be detected, as $5x10^5$ CFUs/ml is the threshold level of *S. mutans* that can best separate healthy individuals from individuals with caries. These results show that the assay is within the clinically relevant range necessary to use concentrations of salivary *S. mutans* for caries diagnosis.

Though this pair of antibodies worked well as a matched pair, reversing their position in the full sandwich could be a better orientation and might even produce a more rounded signal instead of the half-moon shaped signal seen when SWLA-1 is in the capture position. Also, a rounder signal spot makes analysis of the images more reliable.

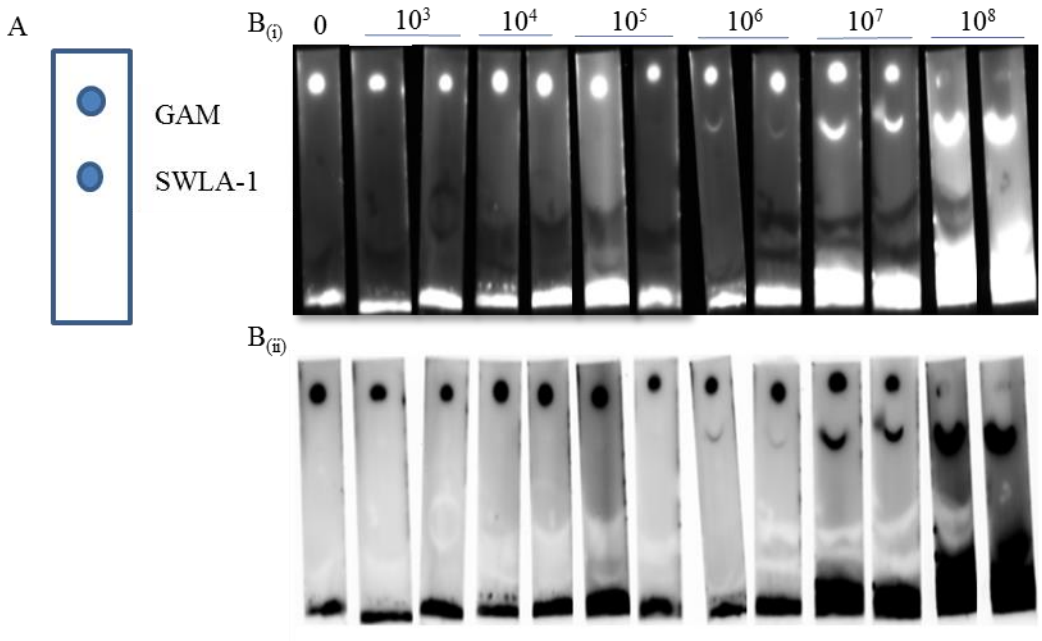


**Figure 10.** Initial Sandwich assay with SWLA-1 as capture and biotin conjugated SWLA-3 as detection antibody using the dipstick format. (A**)** Layout of spotted antibodies and concentrations (B) Resulting images after designated concentration of bacteria ($10^{3}$-$10^{8}$) were run in the assay.

The positive GAM signal seen at the top of all strips in Figure 11B indicates that biotinylation of SWLA-1 was successful, but its antigen recognition was lost in the conjugation process. To determine whether the antibody's reactivity was completely abolished by biotinylation, SWLA-1 and strep-HRP were flowed one after the other so that antibody could bind antigen separate from strep-HRP interacting with the antibody. When antibody and strep-HRP were flowed separately, small faint signals over spots of heat-fixed bacteria were present (Fig. 11B right), but the intensity of the signal is dramatically lower than the signal produced in a half sandwich with unconjugated SWLA-1 (Fig. 8D). These results suggest that biotin molecules maybe attaching in a region of the antibody where antigen recognition occurs. The conjugation method uses EDC NHS chemistry which attaches conjugates to protein through primary amines. Biotin is very small and alone its attachment may not completely eliminate activity towards antigen, but when biotin is in the presence of streptavidin their strong affinity for one another

would likely out compete the antibody-antigen interaction. Since strep-HRP conjugates are fairly large at 100 kilodaltons (kDa),

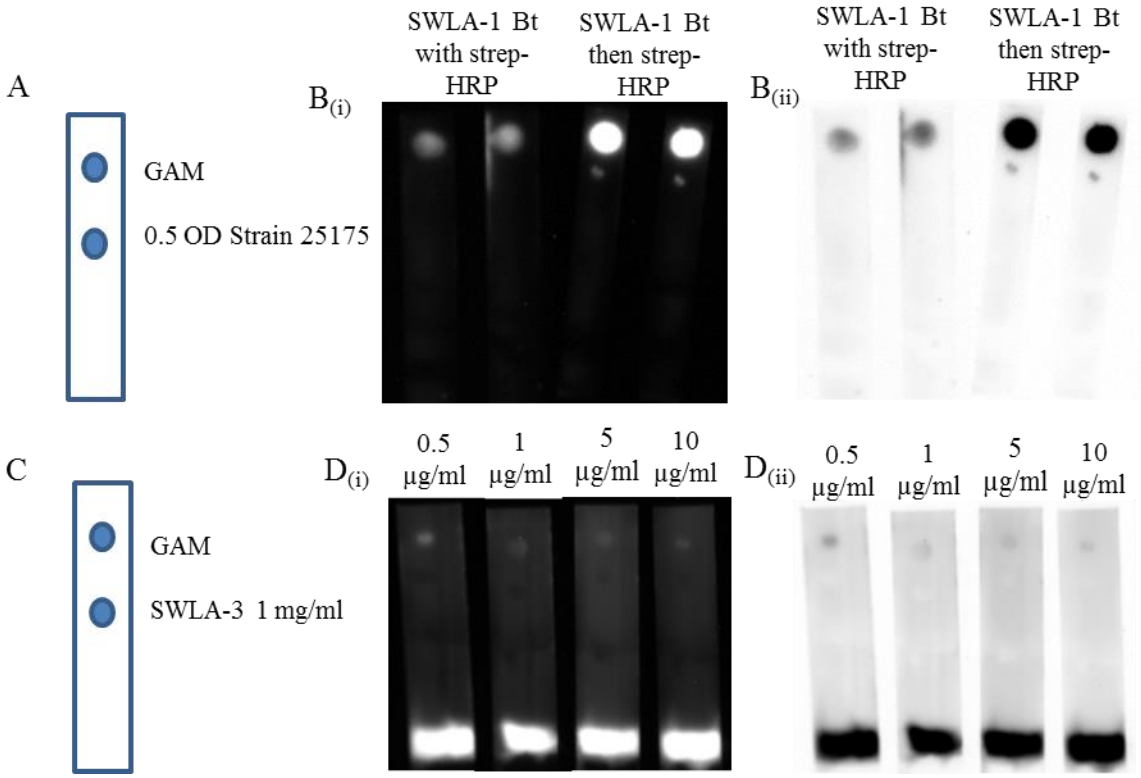


**Figure 11.** Half and full sandwich assays with biotin conjugated SWLA-1 (A) Layout of heat fixed spots on test strip (B) Results of half sandwich assay with biotin conjugated SWLA-1. Biotinylated SWLA-1 was flowed together with streptavidin-HRP (left), or with antibody flowed first then streptavidin-HRP (right). Imaged with 60 second exposure (C) Layout of protein spots on test strips. (D) Results of full sandwich assay run with 1 x $10^7$ CFU/ml (*S. mutans* 25175) and a range of biotinylated SWLA-1 concentrations in the sample buffer, which are listed above the strips. Imaged with 60 second exposure.

the attachment of a molecule that size in an antigen recognition site could interfere with antibody antigen interactions.

In figure 11D, only a faint signal corresponding to the goat anti-mouse positive control spot was produced and no signal was present at the experimental spots where *S. mutans* was to be captured and detected. This result was the same for all detecting antibody (biotinylated SWLA-1) concentrations tested. Optimization of the assay continued with the original orientation, SWLA-1 as capture antibody and biotinylated SWLA-3 as detecting antibody.

## 3.5 Optimization of full sandwich

*Blocking conditions and detergent composition*

Although the purpose of blocking is to prevent non-specific binding, which should reduce background, membranes treated with higher concentrations of BSA tended to have slower flow times, so it was important to find the appropriate concentration of BSA used to block the membranes. In the initial full sandwich experiments (Fig. 10B), a large and intense band was consistently present in the area of the membrane covered by the sample pad. For this reason, pre-treatment of the sample pad with tween20 was also tested with the intent of increasing the number of bacteria that make it to the reaction zone, by improving their flow through the glass fiber and onto the membrane.

Results from test strips with untreated sample pads under all blocking conditions have a circular signal at the top and a half-moon shaped signal just below that (Fig. 12A). The level of background for test strips with untreated sample pads are highest for the unblocked membranes, where the GAM signal is almost of equal intensity (Fig 12A). Strips with untreated sample pads blocked with 1%, 2% or 3% BSA had about the same level of background, but all much lower than the unblocked (Fig. 12A).

Assays run with treated sample pads had higher background overall compared to those run with untreated sample pads (Fig. 12B). Interestingly, for assays run with treated sample pads the increase in BSA used to pre-block the membranes, seems to also increase background. The set of test strips run with treated sample pads also have lower intensity GAM signals than the GAM signals in the set of strips with untreated sample pads.

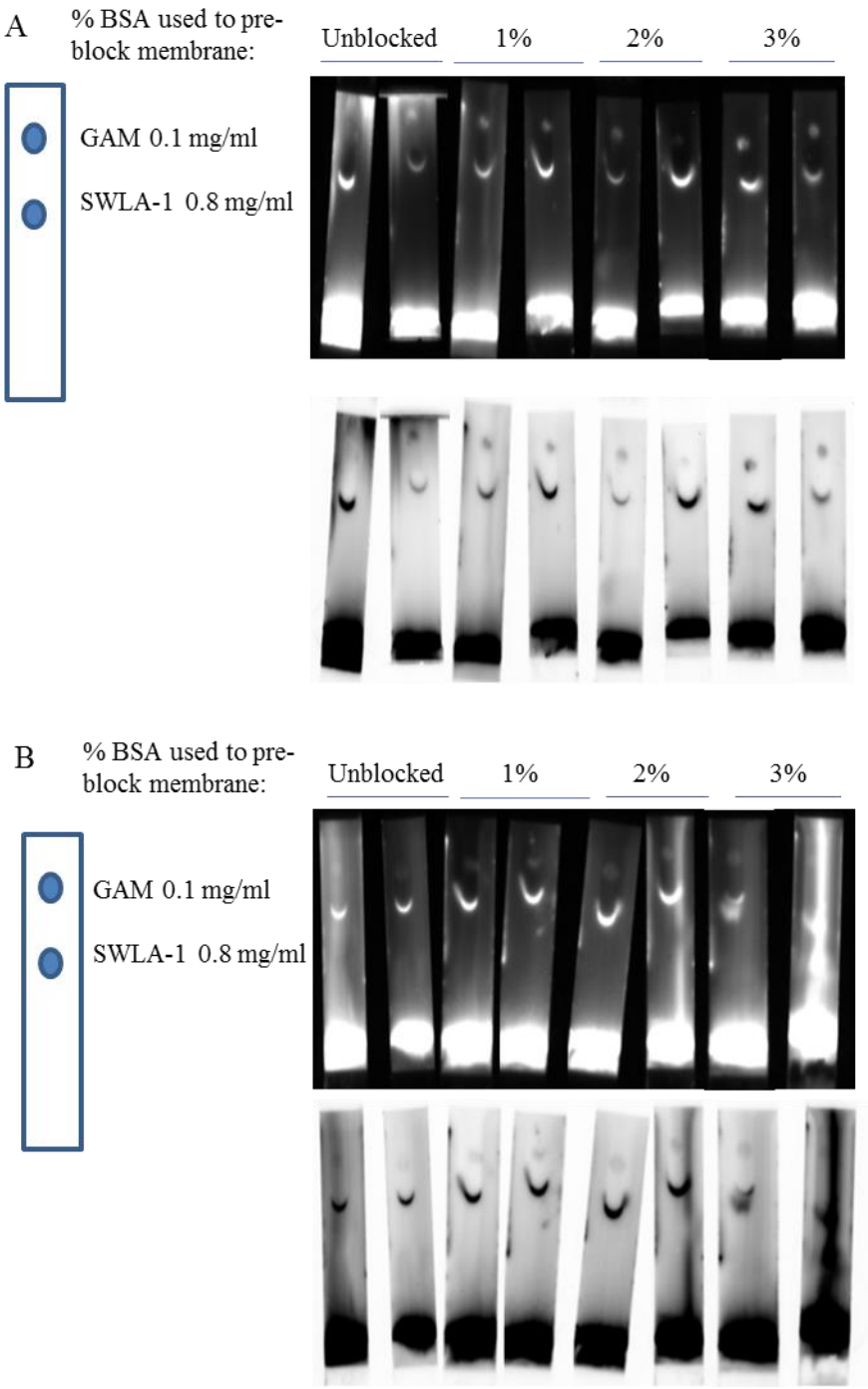


**Figure 12.** Results of running 1 x $10^7$ CFU/ml (*S. mutans* 25175) with a range of BSA concentrations used to pre-block the membranes with and without 1% tween 20 treated sample pads. (A) Images from assays run with untreated sample pads. Imaged with 60 second exposure (B) Images from assays run with 1% tween 20 treated sample pad. Imaged with 60 second exposure

Altering blocking conditions with and without tween20 sample pad treatment indicated that the percentage of BSA used to block the membranes had only a small impact on reducing

background and tween20 treated sample pads increased background (Fig. 12). Since detergents are used to reduce background it was a surprise when tween20 treatment caused dramatically increased background. One explanation for this could be that the detergent treatment prevents strong attachment of the glass fiber to the adhesive, which would negatively impact flow. The increased background associated with tween20 treatment was most apparent when strips were also blocked with the highest BSA content, which suggests slower flow rates contributed to high background levels seen tween 20 treatment. Since *S. mutans* is a chain forming bacteria and this may hinder its flow through the glass fiber sample pad and over the membrane, instead a short pre-incubation in a solution with detergent may improve flow. All subsequent experiments used untreated sample pads and the previous blocking conditions (5 minutes with 1% BSA) were left unchanged.

*Tween 20 composition of sample and wash buffers*

Since the bacteria, strep-HRP, and detection antibodies were incubated in the sample buffer before flowing over the membrane, adding detergent here allows more time for detergent interaction with the bacteria. Samples in previous experiments contained 0.05% tween 20, but a higher detergent concentration may improve flow of bacteria across the membrane by breaking up the chains, altering the cell membrane characteristics such as hydrophobicity, and potentially lysing some cells completely [65, 66].

Results from assays performed with a range of tween20 in the sample buffer and no tween20 in the wash buffer had highly variable background levels (Fig. 13). Test strips that had 0.05% tween 20 in the wash buffer had consistently lower background when the samples were run in buffers containing 0.1% tween 20 or less (Fig 13B). However, even with tween in the wash, backgrounds were high when 0.25% tween 20 was also present in the sample buffer (Fig 13B). Assays that included tween in the wash buffer also had a slightly less intense band under the sample pad.

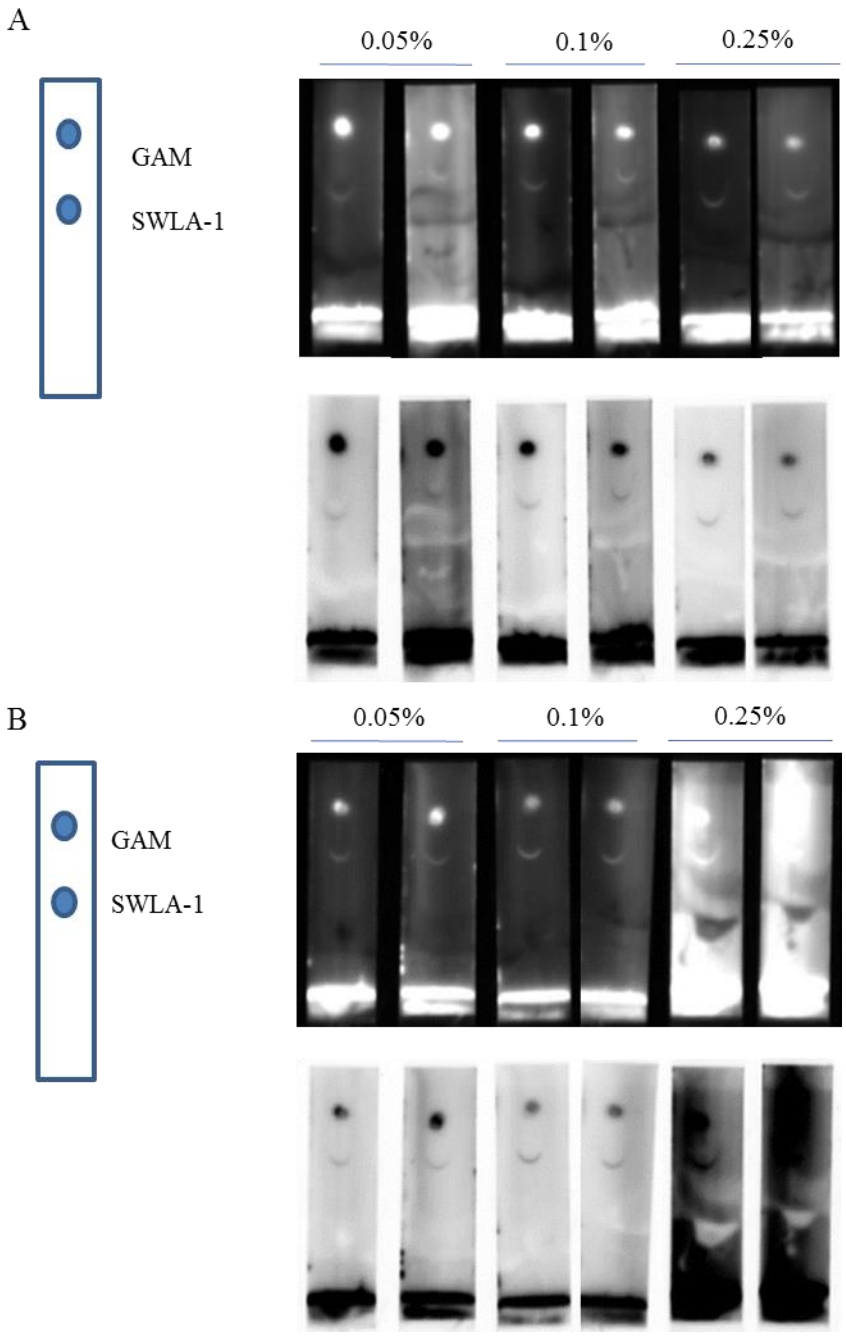


**Figure 13.** Results of running 1 x $10^6$ CFU/ml (*S. mutans* 25175) with a range of tween 20 concentrations in the sample buffer, which are listed above the strips, tested with and without 0.05% tween 20 in the wash buffer. (A) Images from assays run without tween 20 in wash buffer. Imaged with 60 second exposure (B) Images from assays run with tween 20 in wash buffer. Imaged with 60 second exposure.

The total amount of tween20 seems to be a more important factor than whether it's in the sample or wash buffers. However, adding a small amount of tween to the wash buffer did reduce background more consistently than conditions tested with only a PBS wash buffer. The addition of 0.05% tween 20 in the wash buffer was implemented in all future assays and helped to reduce background variability.

## 3.6 Evaluation of analytical performance

In figure 14C, a small round spot corresponding to the GAM positive control spot, just right of center, is present across all test strips. No signal is present over the SWLA-1 capture spot for the negative controls, flowed with no bacteria or concentrations of $5x10^6$ CFU/ml or lower. The lowest concentration tested in which a signal over the S. mutans spot is present is at $5x10^6$ CFUs/ml. The brightness of the spot increased with the concentration of *S. mutans* flowed. This pattern was confirmed through analysis used to create the dose response curve in Fig 14A. The calculated value for the LOB of the assay was determined to be at a concentration of $7.83x10^5$ and the LOD was $2.64\ x10^6$. The LOB is at a high concentration, higher than even the LOD would need to be for the sensitivity to be in the clinical range, but in this data set signal-to-background ratios were very similar with no bacteria as they were with 1,000,000 cells/ml. The calculated LOD on the other hand seems a little lower than expected from visual inspection of the images alone since $5x10^6$ CFUs/ml generated such a weak signal. More testing would be required to determine whether the calculated value of $2.64x10^6$ CFUs/ml is actually the lowest concentration that can be distinguished from the blank in the assays current form. Without a larger number of replicates for analysis it is difficult to establish a meaningful LOD/LOQ.

In previous testing, signals were visible at much lower bacterial concentrations, for which all strips were hand spotted. The volume of capture antibody required to hand spot is much greater than what is dispensed when using an automated spotting system. The total protein

spotted in SWLA-1 capture spots when hand spotted was 0.4 µg/ spot, while automated spotting even with a much more concentrated antibody solution, only resulted in 60 ng total protein per spot. Concentrating the antibody solution further before automated dispensing would increase total antibody available to capture analyte, which may result in increased signal intensity even at lower concentrations.

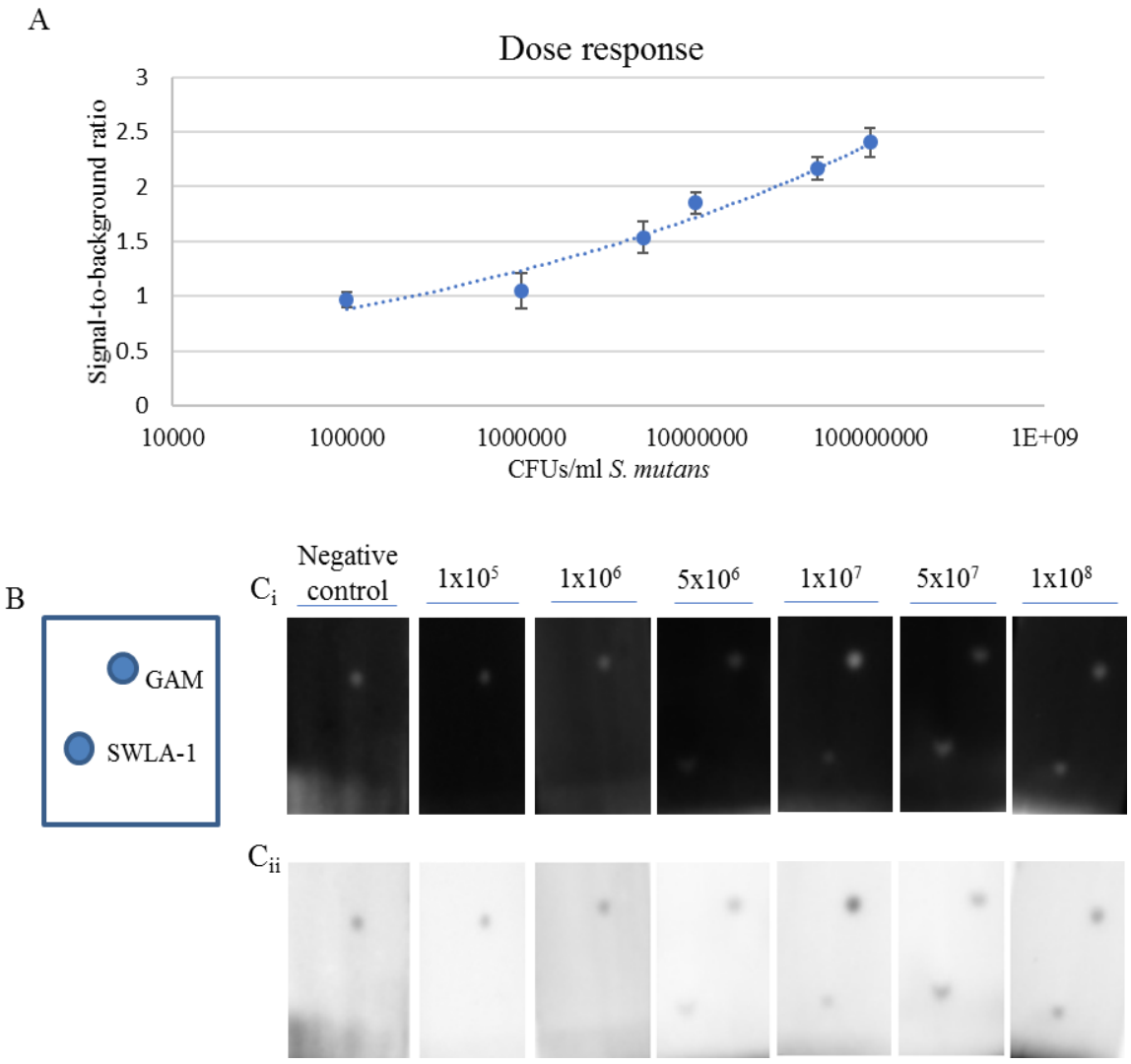


**Figure 14.** Dose response curve. (A) Standard curve for *S. mutans* quantitation based on the signal intensity relative to background. One standard deviation plotted on error bars. (B) Layout of heat-fixed spots on nitrocellulose test strip. (C) Representative images of test strips for each concentration of bacteria tested in the standard curve.

Another crucial factor to consider about this assay compared to the previous experiments in which lower concentrations were detectable is the sample matrix. Saliva contains "sticky" proteins like mucins that help to make saliva viscous and trap bacteria within it [67]. Other salivary components such as endogenous proteases or, salivary antibodies that also target the analyte of interest, could also interfere with the assay [68, 69]. Although all proteins within froze pooled saliva will have undergone a freeze-thaw cycle, this may not completely abolish the structural and functional integrity of all proteins, especially the glycosylated regions of mucins. Even without interference of endogenous proteins the increased viscosity of saliva could slow down kinetics of the assay. Antibody kinetics are directly related to the sensitivity of any immunoassay and a slowed rate of binding would be likely to increase the LOD. The addition of mucolytic agents or protease inhibitors could help reduce viscosity and therefore improve kinetics.

# 4 SUMMARY AND CONCLUSIONS

*S. mutans* is often essential in the development and progression of cavities and a contributor to many other serious systemic diseases. Its rapid detection would prove beneficial in fields outside of dentistry, especially if implemented as a routine diagnostic. Although Diagnostics for detection of *S. mutans* exist, the less time consuming, labor intensive and complex the assay, the more likely it is to be applied as a routine part of modern healthcare.

Detection of both serotype *c* and non-serotype *c S. mutans* in a single assay was the goal initially. Screening of the three SWLA antibodies against the non-serotype *c* strain, 35668, indicated that only SWLA-1 and 2 were able to recognize this strain. Unfortunately, attempts to purify SWLA-2 from cell culture supernatant were not successful so assay development continued by testing purified antibodies SWLA-1 and -3 as a matched pair for detection of a serotype *c* strain, 25175.

The initial dose response with SWLA-1 as the capture antibody and SWLA-3 as the detecting antibody, indicated that these antibodies, in this orientation could not only detect S. mutans, but could detect it under flow at concentrations within the clinical range. Bacterial concentrations tested near the healthy vs. diseased threshold of $5x10^6$, produced only faint signals with a half-moon shape that was not preferable for analysis.

In an attempt to potentially improve upon the initial full sandwich assay, antibody orientation was reversed; SWLA-1 was in the detecting position and SWLA-3 was in the capture position. This required that SWLA-1 be conjugated to biotin. After conjugation SWLA-1 was no longer able to recognize *S. mutans* in the presence of strep-HRP, indicating that the biotin conjugation altered sites important for antigen recognition. Assay development continued by optimizing with SWLA-1 in the capture position and SWLA-3 in the detection position.

To assess analytical performance of the assay, a dose response curve was created by flowing a range *S. mutans* concentrations and plotting the average signal-to-background ratio. The lowest concentration that could be detected was higher than with previous testing, but automated spotting and use of frozen pooled saliva as the sample matrix were likely the reason for the reduction in sensitivity. Increasing capture antibody concentration or adding reagents to reduce the viscosity of samples could lower the LOD.

Future experiments would be focused on first lowering the LOD so that it is within the clinically relevant range, which will require assessment and mitigation of the negative effects frozen pooled saliva has on the assay. This will be an essential step before moving towards a fresh saliva matrix. Future work would also include determining the specificity of the assay across the *S. mutans* species by testing strains from each of the serotype groups as well confirming data from SWLA hybridoma suppliers that indicates a lack of cross-reactivity with other oral pathogens.

## LITERATURE CITED


1. Delahaye, F., et al., *Systematic Search for Present and Potential Portals of Entry for Infective Endocarditis.* J Am Coll Cardiol, 2016. **67**(2): p. 151-8.
2. Petersen, P.E., et al., *The global burden of oral diseases and risks to oral health.* Bull World Health Organ, 2005. **83**(9): p. 661-9.
3. Scarlett, M.I. and L.E. Grant, *Ethical oral health care and infection control.* J Dent Educ, 2015. **79**(5 Suppl): p. S45-7.
4. McNerney, R., *Diagnostics for Developing Countries.* Diagnostics (Basel), 2015. **5**(2): p. 200-9.
5. Sharma, S., et al., *Point-of-Care Diagnostics in Low Resource Settings: Present Status and Future Role of Microfluidics.* Biosensors (Basel), 2015. **5**(3): p. 577-601.
6. Loesche, W.J., *Role of Streptococcus mutans in human dental decay.* Microbiological Reviews, 1986. **50**(4): p. 353-380.
7. Parekh, B.S., et al., *Scaling up HIV rapid testing in developing countries: comprehensive approach for implementing quality assurance.* Am J Clin Pathol, 2010. **134**(4): p. 573-84.
8. Jiang, S., et al., *Salivary Microbiome Diversity in Caries-Free and Caries-Affected Children.* Int J Mol Sci, 2016. **17**(12).
9. Kreth, J., et al., *Role of sucrose in the fitness of Streptococcus mutans.* Oral Microbiol Immunol, 2008. **23**(3): p. 213-9.
10. Banas, J.A. and M.M. Vickerman, *Glucan-binding proteins of the oral streptococci.* Crit Rev Oral Biol Med, 2003. **14**(2): p. 89-99.
11. Guo, L., et al., *The well-coordinated linkage between acidogenicity and aciduricity via insoluble glucans on the surface of Streptococcus mutans.* Sci Rep, 2015. **5**: p. 18015.
12. Nakano, K. and T. Ooshima, *Serotype classification of Streptococcus mutans and its detection outside the oral cavity.* Future Microbiology, 2009. **4**(7): p. 891-902.
13. Seki, M., et al., *Effect of mixed mutans streptococci colonization on caries development.* Oral Microbiol Immunol, 2006. **21**(1): p. 47-52.
14. Samaranayake, L., *Saliva as a diagnostic fluid*.* International Dental Journal, 2007. **57**(5): p. 295-299.
15. Gao, X.L., et al., *Novel and conventional assays in determining abundance of Streptococcus mutans in saliva.* Int J Paediatr Dent, 2012. **22**(5): p. 363-8.
16. Kroes, I., P.W. Lepp, and D.A. Relman, *Bacterial diversity within the human subgingival crevice.* Proc Natl Acad Sci U S A, 1999. **96**(25): p. 14547-52.
17. Williams, R.C. and R.J. Gibbons, *Inhibition of bacterial adherence by secretory immunoglobulin A: a mechanism of antigen disposal.* Science, 1972. **177**(4050): p. 697-9.
18. Kolenbrander, P.E., et al., *Coaggregation: specific adherence among human oral plaque bacteria.* Faseb j, 1993. **7**(5): p. 406-13.
19. Kolenbrander, P.E., *Oral microbial communities: biofilms, interactions, and genetic systems.* Annu Rev Microbiol, 2000. **54**: p. 413-37.
20. Mattila, P.T., et al., *Prevalence and simultaneous occurrence of periodontitis and dental caries.* J Clin Periodontol, 2010. **37**(11): p. 962-7.
21. Dani, S., et al., *Assessment of Streptococcus mutans in healthy versus gingivitis and chronic periodontitis: A clinico-microbiological study.* Contemp Clin Dent, 2016. **7**(4): p. 529-534.
22. Tjaderhane, L., et al., *The activation and function of host matrix metalloproteinases in dentin matrix breakdown in caries lesions.* J Dent Res, 1998. **77**(8): p. 1622-9.

23. Larmas, M., *Dental caries seen from the pulpal side: a non-traditional approach.* J Dent Res, 2003. **82**(4): p. 253-6.
24. Sulkala, M., et al., *Matrix metalloproteinase-8 (MMP-8) is the major collagenase in human dentin.* Arch Oral Biol, 2007. **52**(2): p. 121-7.
25. Hedenbjork-Lager, A., et al., *Caries correlates strongly to salivary levels of matrix metalloproteinase-8.* Caries Res, 2015. **49**(1): p. 1-8.
26. Tannure, P.N. and E.C. Küchler, *Patients With Manifest Caries Lesions Have Higher Levels of Salivary Matrix Metalloproteinase-8 Than Patients With no Caries Lesions.* Journal of Evidence Based Dental Practice, 2016. **16**(1): p. 77-78.
27. Zarella, B.L., et al., *The role of matrix metalloproteinases and cysteine-cathepsins on the progression of dentine erosion.* Arch Oral Biol, 2015. **60**(9): p. 1340-5.
28. Sorsa, T., et al., *Analysis of matrix metalloproteinases, especially MMP-8, in gingival creviclular fluid, mouthrinse and saliva for monitoring periodontal diseases.* Periodontol 2000, 2016. **70**(1): p. 142-63.
29. Mitchell, T.J., *The pathogenesis of streptococcal infections: from tooth decay to meningitis.* Nat Rev Microbiol, 2003. **1**(3): p. 219-30.
30. Kojima, A., et al., *Infection of specific strains of Streptococcus mutans, oral bacteria, confers a risk of ulcerative colitis.* Scientific Reports, 2012. **2**.
31. Gronroos, L. and S. Alaluusua, *Site-specific oral colonization of mutans streptococci detected by arbitrarily primed PCR fingerprinting.* Caries Res, 2000. **34**(6): p. 474-80.
32. Waterhouse, J.C. and R.R. Russell, *Dispensable genes and foreign DNA in Streptococcus mutans.* Microbiology, 2006. **152**(Pt 6): p. 1777-88.
33. Watanabe, I., et al., *Oral Cnm-positive Streptococcus Mutans Expressing Collagen Binding Activity is a Risk Factor for Cerebral Microbleeds and Cognitive Impairment.* Sci Rep, 2016. **6**: p. 38561.
34. Nakano, K., et al., *Roles of oral bacteria in cardiovascular diseases--from molecular mechanisms to clinical cases: Cell-surface structures of novel serotype k Streptococcus mutans strains and their correlation to virulence.* J Pharmacol Sci, 2010. **113**(2): p. 120-5.
35. Kojima, A., et al., *Infection of specific strains of Streptococcus mutans, oral bacteria, confers a risk of ulcerative colitis.* Sci Rep, 2012. **2**: p. 332.
36. Nakano, K., R. Nomura, and T. Ooshima, *Streptococcus mutans and cardiovascular diseases.* Japanese Dental Science Review, 2008. **44**(1): p. 29-37.
37. Nakano, K., et al., *The collagen-binding protein of Streptococcus mutans is involved in haemorrhagic stroke.* Nat Commun, 2011. **2**: p. 485.
38. Nomura, R., et al., *Contribution of the interaction of Streptococcus mutans serotype k strains with fibrinogen to the pathogenicity of infective endocarditis.* Infect Immun, 2014. **82**(12): p. 5223-34.
39. Nomura, R., K. Nakano, and T. Ooshima, *Contribution of glucan-binding protein C of Streptococcus mutans to bacteremia occurrence.* Arch Oral Biol, 2004. **49**(10): p. 783-8.
40. Lockhart, P.B., et al., *Bacteremia associated with toothbrushing and dental extraction.* Circulation, 2008. **117**(24): p. 3118-25.
41. Nakano, K., et al., *Contribution of biofilm regulatory protein A of Streptococcus mutans, to systemic virulence.* Microbes Infect, 2005. **7**(11-12): p. 1246-55.
42. Brown, M. and G.E. Griffin, *Immune responses in endocarditis.* Heart, 1998. **79**(1): p. 1-2.
43. Nakano, K., et al., *Detection of cariogenic Streptococcus mutans in extirpated heart valve and atheromatous plaque specimens.* J Clin Microbiol, 2006. **44**(9): p. 3313-7.

44. Chhibber-Goel, J., et al., *Linkages between oral commensal bacteria and atherosclerotic plaques in coronary artery disease patients.* npj Biofilms and Microbiomes, 2016. **2**(1).
45. Vasovic, M., et al., *The relationship between the immune system and oral manifestations of inflammatory bowel disease: a review.* Cent Eur J Immunol, 2016. **41**(3): p. 302-310.
46. Kesavalu, L., et al., *Increased atherogenesis during Streptococcus mutans infection in ApoE-null mice.* J Dent Res, 2012. **91**(3): p. 255-60.
47. Nakano, K., et al., *Serotype distribution of Streptococcus mutans a pathogen of dental caries in cardiovascular specimens from Japanese patients.* J Med Microbiol, 2007. **56**(Pt 4): p. 551-6.
48. Soell, M., et al., *Activation of human monocytes by streptococcal rhamnose glucose polymers is mediated by CD14 antigen, and mannan binding protein inhibits TNF-alpha release.* J Immunol, 1995. **154**(2): p. 851-60.
49. Chia, J.S., et al., *Platelet aggregation induced by serotype polysaccharides from Streptococcus mutans.* Infect Immun, 2004. **72**(5): p. 2605-17.
50. Abranches, J., et al., *The collagen-binding protein Cnm is required for Streptococcus mutans adherence to and intracellular invasion of human coronary artery endothelial cells.* Infect Immun, 2011. **79**(6): p. 2277-84.
51. Shun, C.T., et al., *Activation of human valve interstitial cells by a viridians streptococci modulin induces chemotaxis of mononuclear cells.* J Infect Dis, 2009. **199**(10): p. 1488-96.
52. Yeh, C.Y., J.Y. Chen, and J.S. Chia, *Glucosyltransferases of viridans group streptococci modulate interleukin-6 and adhesion molecule expression in endothelial cells and augment monocytic cell adherence.* Infect Immun, 2006. **74**(2): p. 1273-83.
53. Matsumoto-Nakano, M., et al., *Contribution of cell surface protein antigen c of Streptococcus mutans to platelet aggregation.* Oral Microbiology and Immunology, 2009. **24**(5): p. 427-430.
54. Nagata, E. and T. Oho, *Invasive Streptococcus mutans induces inflammatory cytokine production in human aortic endothelial cells via regulation of intracellular toll-like receptor 2 and nucleotide-binding oligomerization domain 2.* Mol Oral Microbiol, 2017. **32**(2): p. 131-141.
55. Tonomura, S., et al., *Intracerebral hemorrhage and deep microbleeds associated with cnm-positive Streptococcus mutans; a hospital cohort study.* Sci Rep, 2016. **6**: p. 20074.
56. Brito, F., et al., *Prevalence of periodontitis and DMFT index in patients with Crohn's disease and ulcerative colitis.* J Clin Periodontol, 2008. **35**(6): p. 555-60.
57. Szymanska, S., et al., *Dental caries, prevalence and risk factors in patients with Crohn's disease.* PLoS One, 2014. **9**(3): p. e91059.
58. Kojima, A., et al., *Aggravation of inflammatory bowel diseases by oral streptococci.* Oral Dis, 2014. **20**(4): p. 359-66.
59. Low, S.C., et al., *Electrophoretic interactions between nitrocellulose membranes and proteins: Biointerface analysis and protein adhesion properties.* Colloids Surf B Biointerfaces, 2013. **110**: p. 248-53.
60. Shi, W. and W.R. Hume, *Antibodies to S. mutans and uses thereof*. 2001, Google Patents.
61. Ajdic, D., et al., *Genome sequence of Streptococcus mutans UA159, a cariogenic dental pathogen.* Proc Natl Acad Sci U S A, 2002. **99**(22): p. 14434-9.
62. Armbruster, D.A. and T. Pry, *Limit of blank, limit of detection and limit of quantitation.* Clin Biochem Rev, 2008. **29 Suppl 1**: p. S49-52.
63. *Evaluation of Detection Capability for Clinical Laboratory Measurement Procedures, 2nd Edition*, in *EP17-A2*. 2012. p. 80.

64. *The Immunoassay Handbook*, D. Wild, Editor. 2013, Elsevier Science.
65. Russell, A.D., *Antibiotic and biocide resistance in bacteria: introduction.* J Appl Microbiol, 2002. **92 Suppl**: p. 1s-3s.
66. Liaqat, I. and A.N. Sabri, *Analysis of cell wall constituents of biocide-resistant isolates from dental-unit water line biofilms.* Curr Microbiol, 2008. **57**(4): p. 340-7.
67. Thomadaki, K., et al., *Whole-saliva proteolysis and its impact on salivary diagnostics.* J Dent Res, 2011. **90**(11): p. 1325-30.
68. Frenkel, E.S. and K. Ribbeck, *Salivary mucins protect surfaces from colonization by cariogenic bacteria.* Appl Environ Microbiol, 2015. **81**(1): p. 332-8.
69. Madhwani, T. and A.J. McBain, *The Application of Magnetic Bead Selection to Investigate Interactions between the Oral Microbiota and Salivary Immunoglobulins.* PLoS One, 2016. **11**(8): p. e0158288.